P-04-52

Oskarshamn site investigation

Reflection seismic studies on Ävrö and Simpevarpshalvön, 2003

Christopher Juhlin, Björn Bergman, Hans Palm and Ari Tryggvason
Uppsala University

April 2004

Svensk Kärnbränslehantering AB
Swedish Nuclear Fuel
and Waste Management Co
Box 5864
SE-102 40 Stockholm Sweden
Tel 08-459 84 00
+46 8 459 84 00
Fax 08-661 57 19
+46 8 661 57 19

ISSN 1651-4416
SKB P-04-52

Oskarshamn site investigation

Reflection seismic studies on Ävrö and Simpevarpshalvön, 2003

Christopher Juhlin, Björn Bergman, Hans Palm and Ari Tryggvason
Uppsala University

April 2004

Keywords: Reflection seismics, Reflectors, Bedrock, Overburden, Structures, Fracture zones, Mafic lenses.

Abstract

Reflection seismic data were acquired in the fall of 2003 in the Oskarshamn area, located about 300 km south of Stockholm, Sweden. The Oskarshamn area has been targeted by SKB as a possible storage site for high level radioactive waste. About 3.7 km of high resolution seismic data were acquired along three separate profiles varying in length from 0.8 to 1.9 km. Nominal source and receiver spacing was 10 m with at least 100 active channels when recording data from a dynamite source (15–75 g). All shots were also recorded into a 10 × 20 channel (200 total) fixed array nearly centred over the KAV04 borehole. In addition, about 100 shots were fired within in the array, providing limited 3D coverage below the array.

Both the reflection seismic data and array data indicate several E-W striking reflectors on the island of Ävrö, some of which can be correlated to topographic and magnetic lows. The reflection data indicate that these E-W striking reflectors dip at about 25–50º to the south. A clear south dipping reflector, also imaged on an earlier survey, projects into the KAV04 borehole at 630 m depth. In addition, there are reflectors which dip at 20–50º to the northwest that project up to the surface offshore of the island of Ävrö and parallel (SW-NE) to its coast. The strongest and most clear of these reflectors projects into the KAV04 borehole below 1000 m, below the planned bottom of the well. Both these sets are interpreted as representing possible fracture zones. A strong sub-horizontal reflector at about 700 m depth below the centre of the island of Ävrö may be a mafic lens. It projects into the KAV04 borehole at about this depth. Weaker sub-horizontal reflections may originate from fracture zones, but these have not been well imaged. There are a few strong gently dipping reflections along the profiles that cannot be oriented. Data from the Simpevarp peninsula are difficult to interpret due to the low fold and limited offset range of the acquisition. Therefore the orientation of these reflectors is less well constrained in this area. However, both the E-W striking and SW-NE striking sets of reflectors appear to be present below the Simpevarp peninsula.

Sammanfattning

Reflektionsseismiska data registrerades hösten 2003 i Oskarshamnsområdet, ca 300 km söder om Stockholm. Oskarshamnsområdet är en av platserna SKB har valt att undersöka för möjlig förvaring av hög aktivt kärnavfall. Ca 3,7 km av högupplösande reflektionsseismiska data samlades in längs tre separata profiler med varierande längd från 0,8 till 1,9 km. Nominella käll- och mottagaravstånd var 10 m med minst 100 aktiva kanaler. 15–75 g dynamit användes som källa. Alla skott registrerades också på en fast grid (array) (10 × 20 kanaler) som var nästan centrerat över kärnborrhålet KAV04. Ytterligare ca 100 skott sköts inom denna array, vilket gav en begränsad 3D täckning under arrayen.

Både profil- och arraydata indikerar ett flertal O-V strykande strukturer på Ävrö, en del av dessa kan korreleras med topografiska och magnetiska minimum. Reflektionsseismiska data indikerar att dessa zoner stupar 20–50º mot söder. En tydlig stupande reflektor mot syd, vilken också har setts på en tidigare genomförd mätning på Ävrö, tolkas att korsa kärnborrhålet KAV04 på 630 m djup. Dessutom, finns det tydliga reflektorer som stupar 20–50º mot nordväst. Dessa kan projiceras upp till ytan i havet och stryker (SV-NO) parallellt med kusten av Ävrö. Den starkaste och tydligast av dessa projiceras in mot kärnborrhålet KAV04 under 1000 m, alltså djupare än borrhålets planerade borrdjup. Båda dessa reflektorer tolkas som sprickzoner. En stark reflektor på ca 700 m djup under mitten av Ävrö kan var en mafisk lins. Den korsar kärnborrhålet KAV04 vid ungefär detta djup. Svagare subhorisontella reflektioner kan härstamma från sprickzoner, men tydliga bilder av dessa har inte erhållits. Det finns några få stupande reflektioner som inte kan orienteras. Data från Simpevarpshalvön är svåra att tolka på grund av den låga faltningen ”fold” och begränsat avstånd mellan källa och mottagare. Orienteringen av reflektorerna är därför oviss i detta område. Men, både O-V och SV-NO strykande reflektorer syns under Simpevarpshalvön.

Contents

1 Introduction

Seismic data were acquired in the Oskarshamn area in southeastern Sweden (Figure 1-1) during the month of November in the year 2003 by Uppsala University in agreement with the instructions and guidelines from SKB (activity plan AP PS 400-03-068 and method description SKB MD 241.004, SKB internal controlling documents) and under supervision of Leif Stenberg, SKB. Approximately 3.7 km of high-resolution (10 m shot and receiver spacing) reflection seismic data were acquired the SERCEL 408UL system along 3 different profiles (Figure 1-2) using about 300 shot points. Most of these shots were also recorded on a SERCEL 348 a stationary array (GSM000010) of 200 channels laid out in a 10 × 20 channel pattern (Figure 1-2). In addition, about 100 shots were fired within the array (GSM000010) itself and recorded both within the array (GSM000010) and along profile 4 (LSM000198) and the northern part of profile 3 (LSM000197).

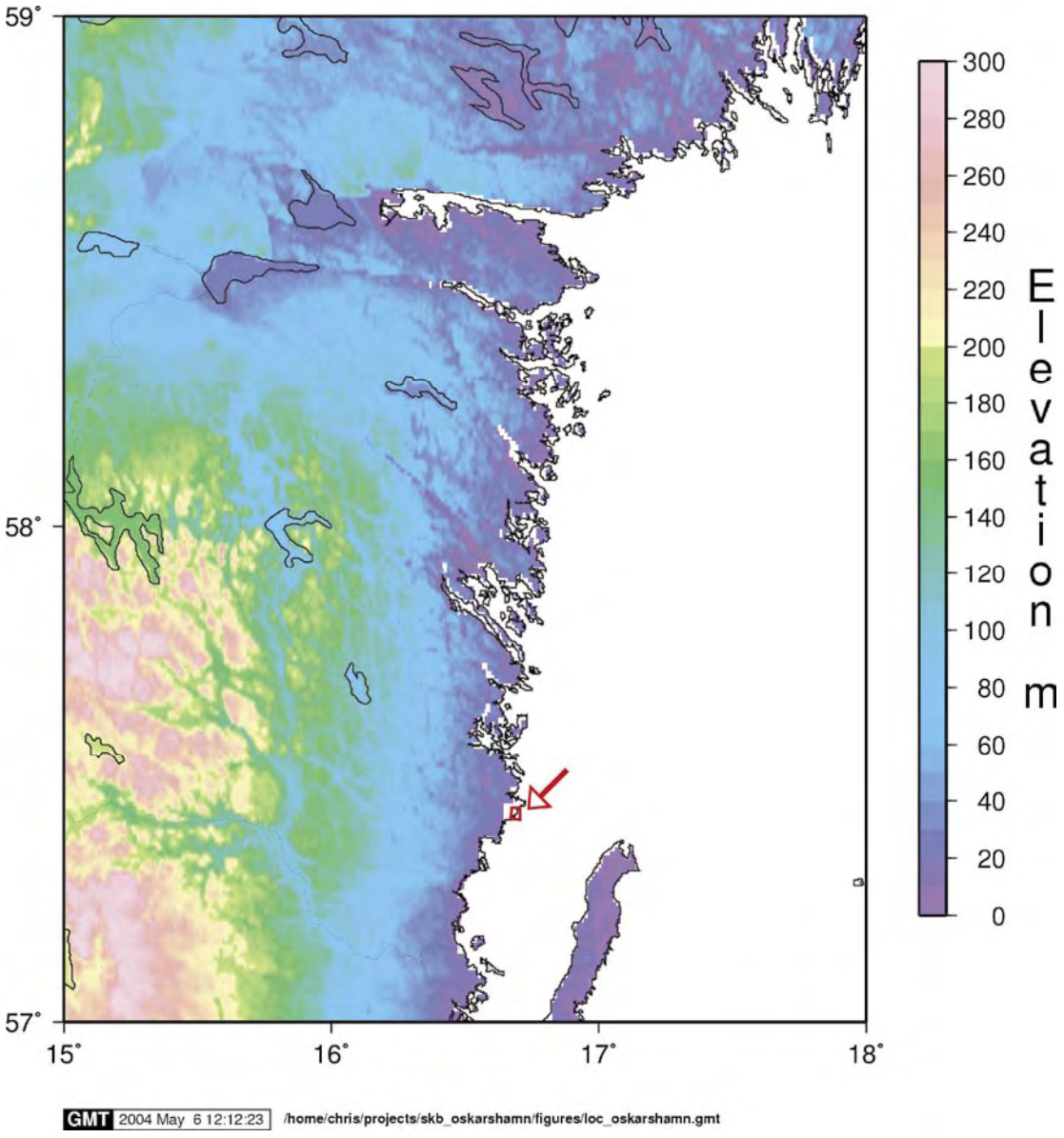

Figure 1-1. *Location of study area (red box marked by arrow).*

Figure 1-2. *Location of the seismic reflection profiles, profile 3, LSM000197, profile 4, LSM000198 and profile 5, LSM000199 (red lines), and the fixed array, GSM000010 (green dots). Also shown are the reflection seismic profiles acquired in 1996 (grey lines) which have been reported in /6,7/ and /3,4/.*

The reflection seismic method used here imaged the bedrock from the near surface (upper 100 metres) down to depths of several km. Zones or changes in the elastic properties of the bedrock, i.e. lithological changes or possible fracture zones, greater than about a metre in thickness and dipping up to 60–70º can be imaged. First arrival picks from the fixed array (GSM000010) were used to determine the uppermost bedrock velocity below and near the array. Shots fired within the array (GSM000010) will provide some 3D information on reflectors below the array.

2 Data acquisition

The acquisition crew arrived in the field on November 10 and data acquisition began on November 16, 2003 using the acquisition parameters given in Table 2-1. There was an approximately 3 day delay in starting acquisition due to that drilling of shot holes had not progressed as far as required. Data acquisition finished on November 26, 2003 followed by 3 days of demobilization and clean-up. During the acquisition period there were 2 days that no data were acquired due to moving of profiles.

Shot points and geophones were located as much as possible on bedrock. Shot holes were drilled at the closest suitable location to a staked point where bedrock was present, but not further from the staked point than 30 cm parallel and 1 m perpendicular to the profile. If no bedrock was found within this area, even after removing 50 cm of soil, the shot hole was drilled at the staked point. In bedrock, 12 mm diameter shot holes were drilled to 90 cm depth with an electric drilling machine powered by a gasoline generator. Charges of 15 g were used in bedrock shot holes. In soil cover, 22 mm diameter shot holes were drilled to 150 cm depth with an air pressure drill. These holes were cased with a plastic casing with an inner diameter of 18 mm. Charges of 75 g were used in these holes. Bedrock shot holes were used on about 50 % of the profiles. Geophones were placed in drilled bedrock holes wherever possible, otherwise they were placed directly in the soil cover. All shot holes and geophone locations were surveyed with high precision GPS instruments in combination with a total station. This combination gave a horizontal and vertical precision of better than 10 cm.

Table 2-1. Acquisition parameters for the reflection and tomographic seismic components.

Parameter	Reflection	Array
Spread type	Shoot through	Fixed array
Number of channels	Minimum 100 Maximum 232	200 with 100 active for recording
Near offset	20 m	20 m
Geophone spacing	10 m	20 m
Line spacing		40 m
Geophone type	28 Hz single	6 × 10 Hz bunch
Shot spacing	10 m	40 m average
Charge size	15/75 gram	15/75 gram
Nominal charge depth	0.9/1.5 m	0.9/1.5 m
Nominal fold	50	12 in 40 m × 20 m bins
Recording instrument	SERCEL 408	SERCEL 348
Sample rate	0.5 ms	1 ms
Field low cut	Out	Out
Field high cut	500 Hz	250 Hz
Record length	3 seconds	3 seconds
Profile length / shots	3– 1850 m / 159 4– 1060 m / 100 5– 770 m / 35 Array- 400 m × 400 m / 100	

Profile 4 (LSM000198) was acquired first followed directly by the firing shots within the array (GSM000010). During acquisition of profile 4 (LSM000198) data were also recorded on stations 3046–3174 on profile 3 (LSM000197), whenever possible. Profile 4 (LSM000198) was then picked up and moved to the southern part of profile 3 (LSM000197) and part of profile 5 (LSM000199). Profile 3 (LSM000197) was then shot with data being recorded along the entire profile as well as on stations 5013–5051 on profile 5 (LSM000199). Stations north of 3150 on profile 3 (LSM000197) were then moved to profile 5 (LSM000199). Profile 5 (LSM000199) was shot with data being recorded along the entire profile and on stations 3001–3150 on profile 3 (LSM000197).

3 Data processing

3.1 Reflection seismic processing

The reflection seismic data were acquired along crooked lines. CDP stacking lines were chosen that were piece-wise straight. The data were projected on to the profiles prior to stacking (Figure 3-1). The stacks shown in this report refer to the CDP numbers along these profiles. The reflection seismic data were processed with the parameters given in Table 3-1. Important processing parameters were refraction statics along with deconvolution and filtering (Figure 3-2).

Since about 100 shots were fired within in the array (GSM000010) it is possible to obtain a limited 3D image below the array. Results from this processing will be presented in a report in June 2004.

Table 3-1. Processing parameters for the seismic profiles.

Step	Process
1	Read SEGD data – 3000 ms
2	Spike and noise edit
3	Pick first breaks
4	Scale by time
5	Surface consistent spiking deconvolution Design gate 0 m: 200–500 ms, 500 m: 350–600 ms, 1800 m: 600–900 ms Operator 60 ms White noise added 1%
6	Bandpass filter 70–140–300–450 Hz 0–100 ms 60–120–300–450 Hz 50–200 ms 40–80–240–360 Hz 150–500 ms 40–80–240–360 Hz 400–700 ms 35–70–180–240 Hz 600–2000 ms
7	Refraction statics
8	Trace top mute: 5 + offset / 5.5 ms
9	Sort to CDP domain
10	Velocity analyses
11	Residual statics
12	Sort to common offset domain
13	AGC – 50 ms window
14	NMO
15	Common offset F-K DMO Average 1D NMO velocity after DMO
16	AGC – 50 ms window
17	Iterative DMO velocity analysis
18	Stack (mean)
19	Trace equalization 0–800 ms
20	F-X Decon
21	Migration

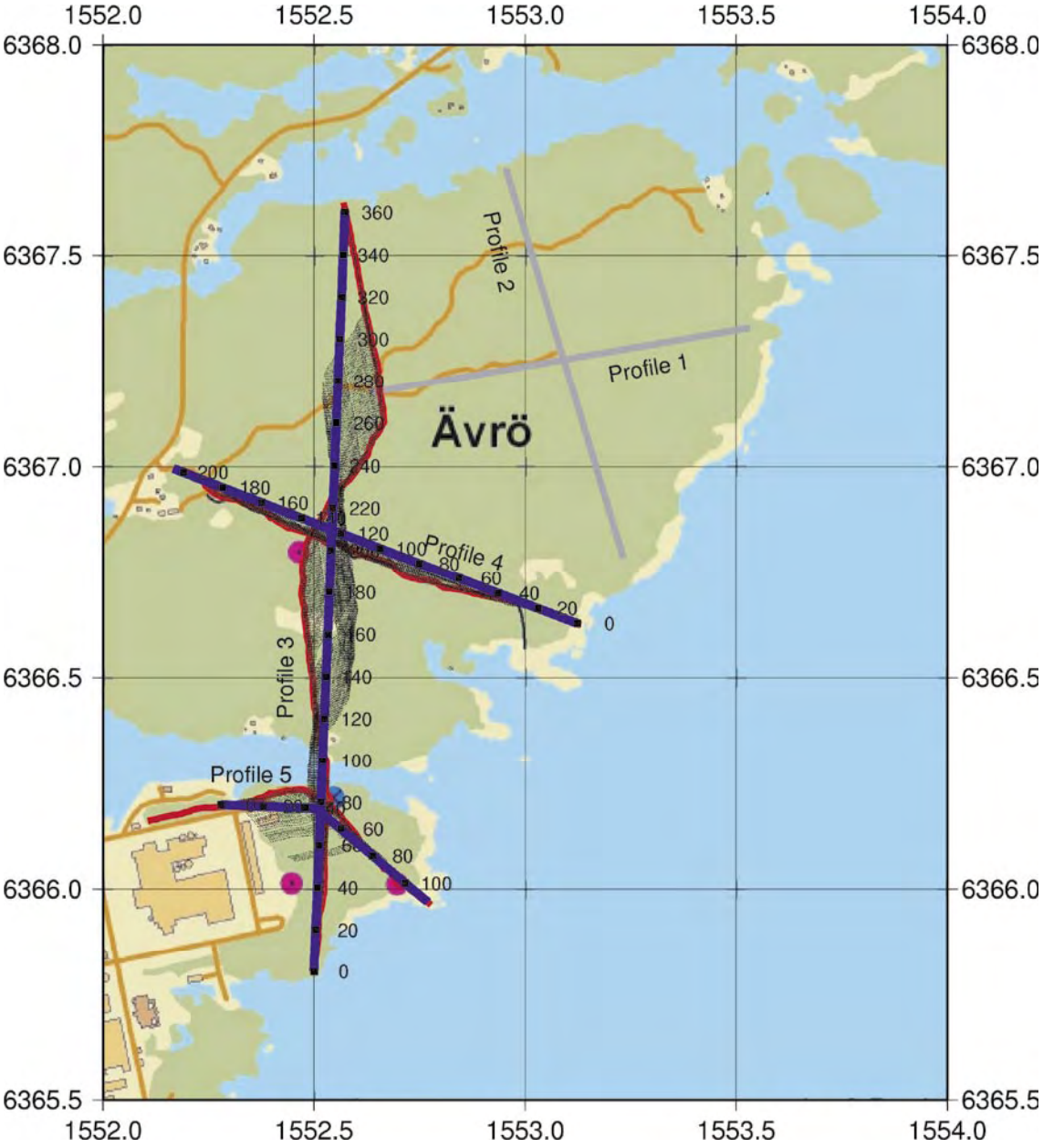

Figure 3-1. *Midpoints between shots and receivers (black dots) used in the processing and the CDP lines that the data have been projected onto and stacked along (blue). Numbering refers to CDP position along the stacking line. Actual location of the seismic profiles (red) are also shown, profile 3 (LSM000197), profile 4 (LSM00198) and profile 5 (LSM000199).*

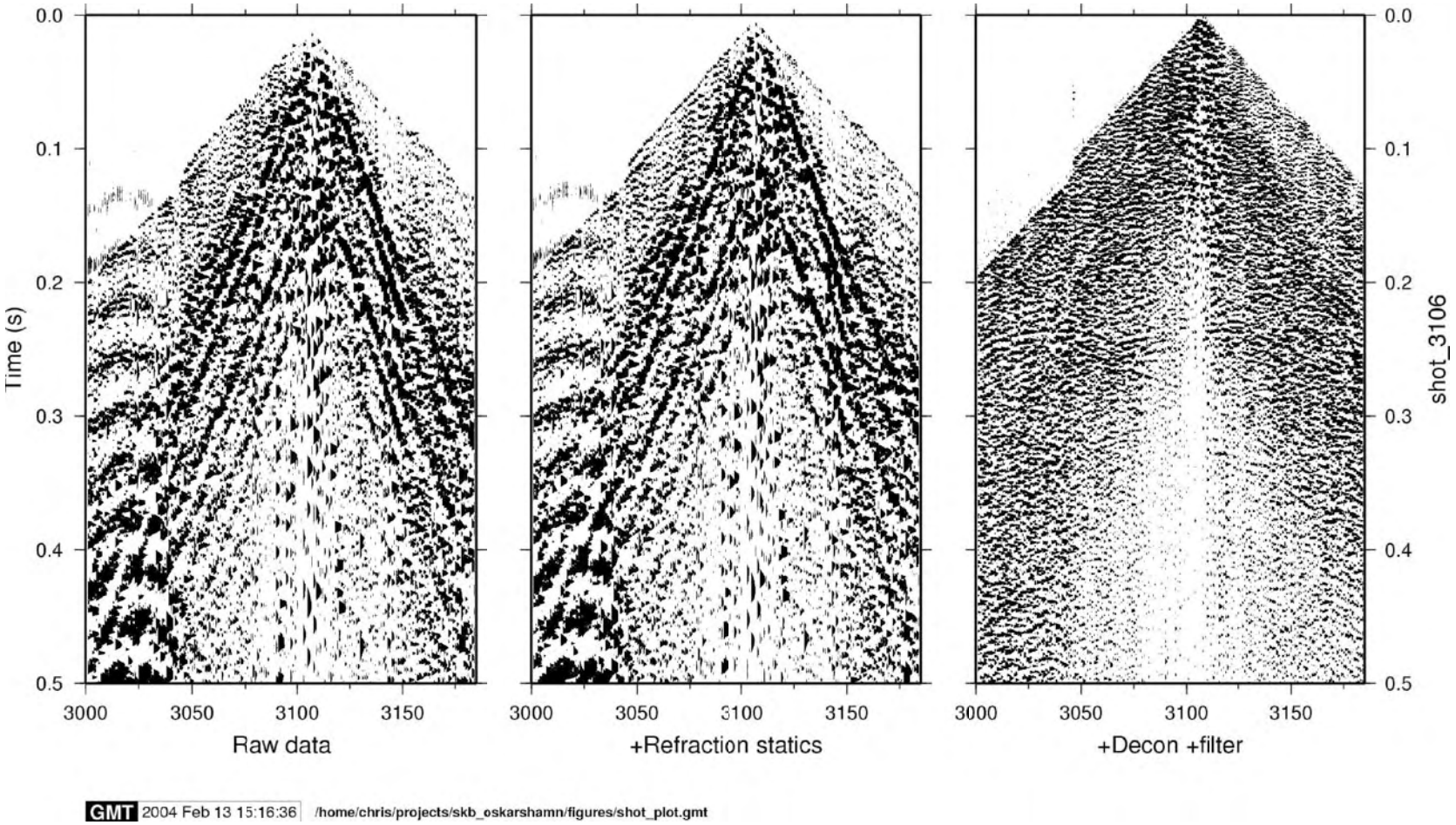

Figure 3-2. *Example of a shot gather from profile 3 (LSM000197) showing raw data scaled by time, with refraction statics added, and after deconvolution and filtering.*

3.2 Stacked and migrated sections

In the figures that follow (Figures 3-3 to 3-8) stacked sections down to 1.6 seconds are first shown followed by a more detailed image of the uppermost 0.5 s for each profile. In these figures the data have been processed to step 20 in Table 3-1. However, DMO has not been applied to profile 5 (LSM000199) due to the poorer signal to noise ratio on this profile.

Profiles 3 (LSM000197) and 4 (LSM000198) have been migrated (Figures 3-9 and 3-10). The reader should keep in mind that many of the reflections are from out of the plane of the profile and therefore the migrated sections cannot be regarded as vertical slices below the profiles. Instead the depth scale should be regarded as distance from the surface to the reflector. The approximate depth scale shown in the figures is based on the average DMO velocity and is only valid for reflections striking perpendicular to the plane of the profile. Since many of the reflections appear to strike E-W (see chapter 4), the migrated image of profile 3 (LSM000197) is reasonably realistic.

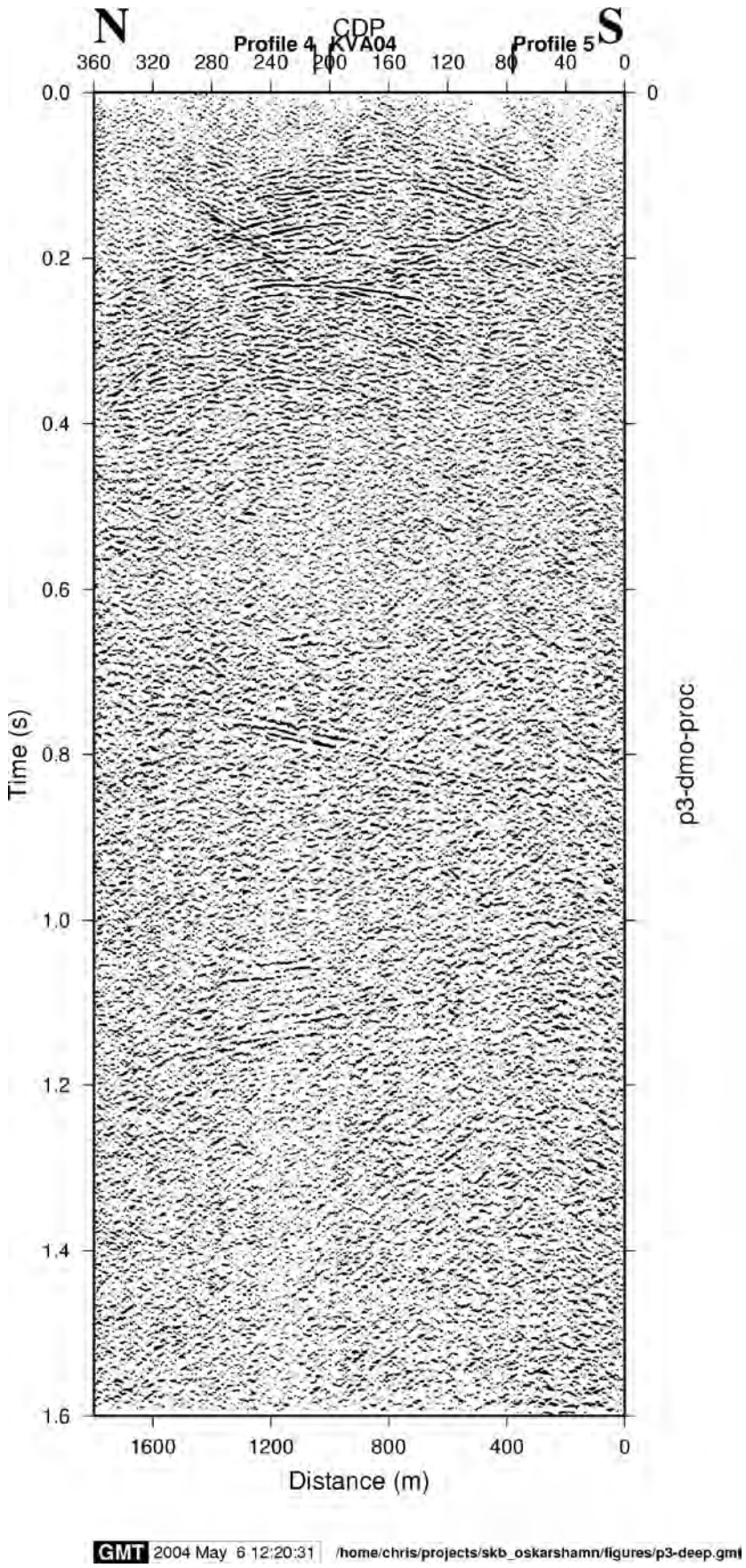

Figure 3-3. *Stacked section of profile 3 (LSM000197) down to 1.6 seconds.*

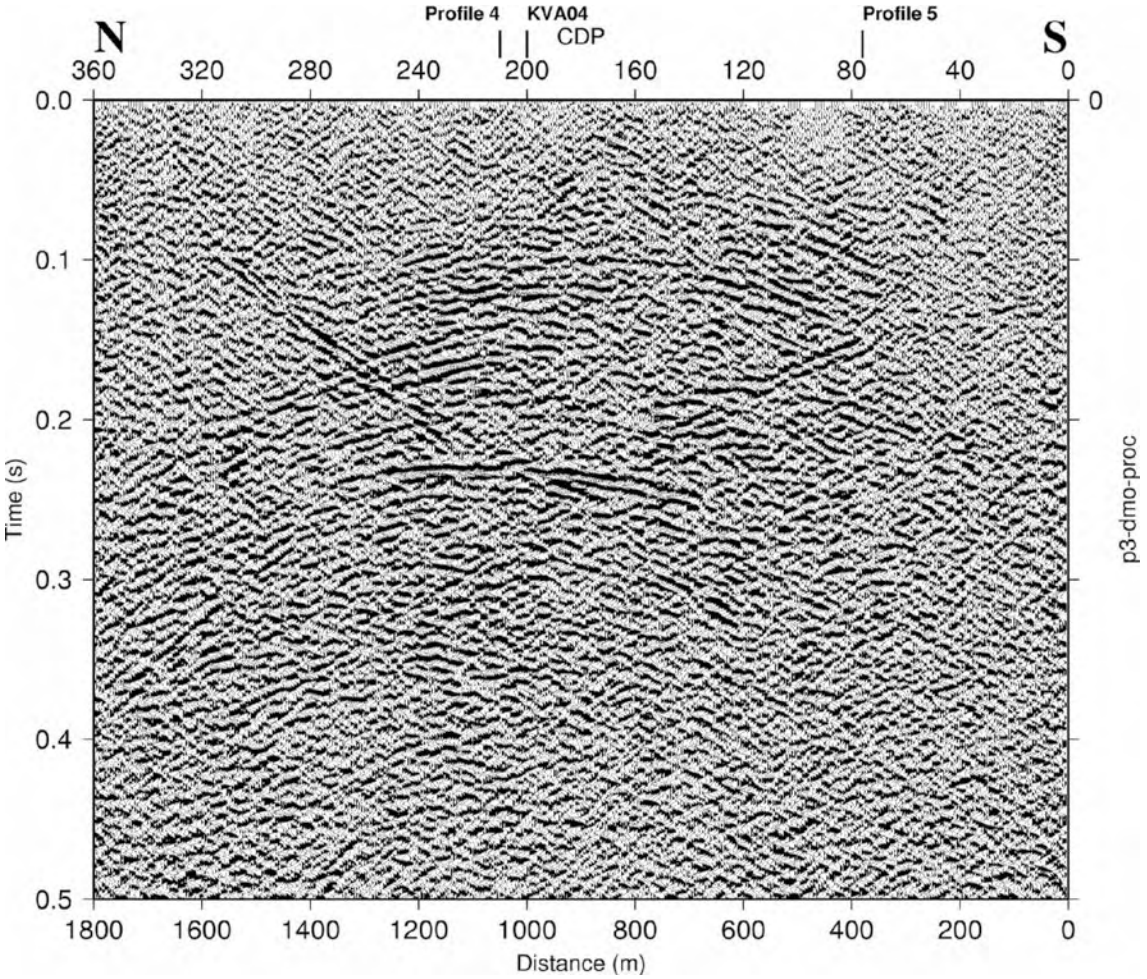

Figure 3-4. *Stacked section of profile 3 (LSM000197) down to 0.5 seconds.*

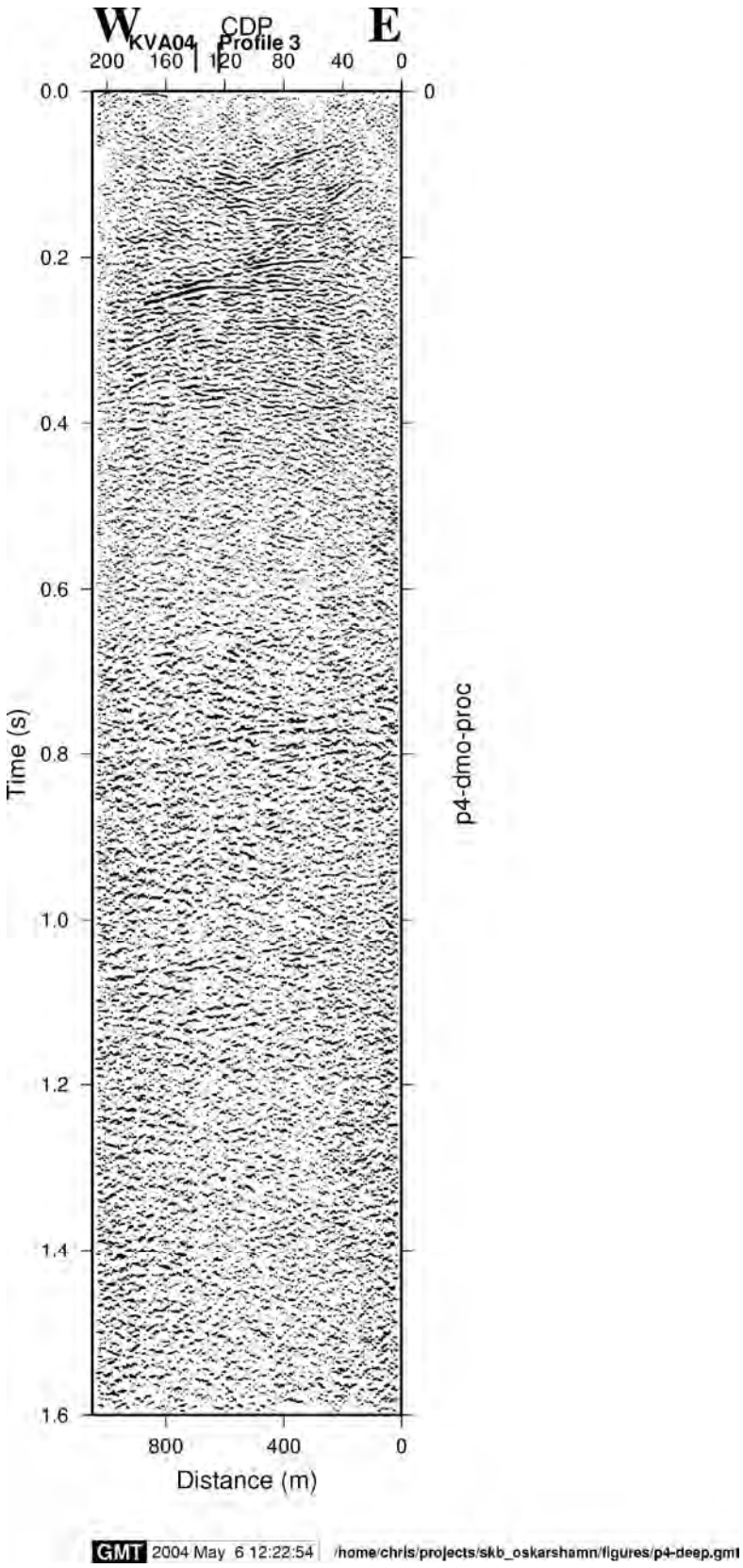

Figure 3-5. *Stacked section of profile 4 (LSM000198) down to 1.6 seconds.*

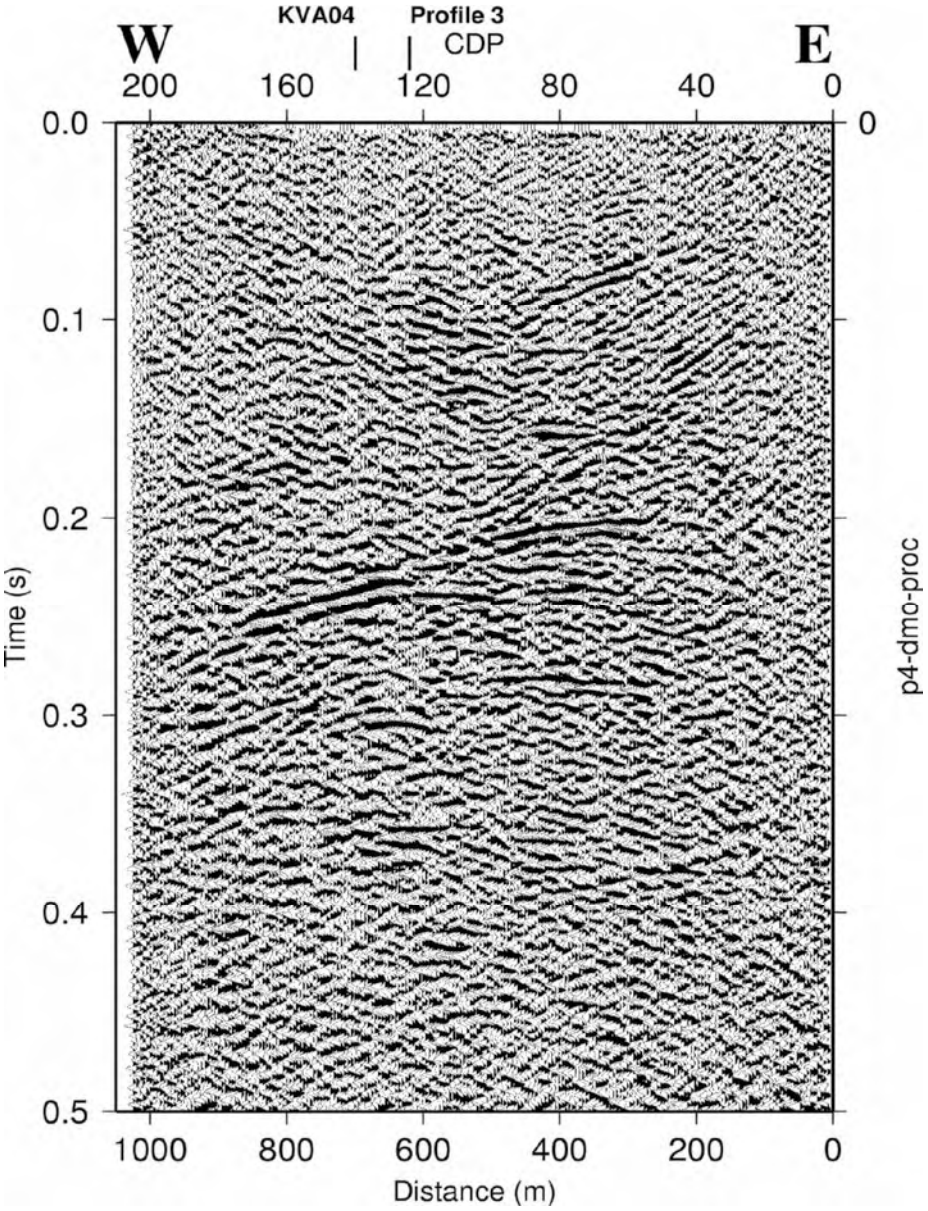

Figure 3-6. *Stacked section of profile 4 (LSM000198) down to 0.5 seconds.*

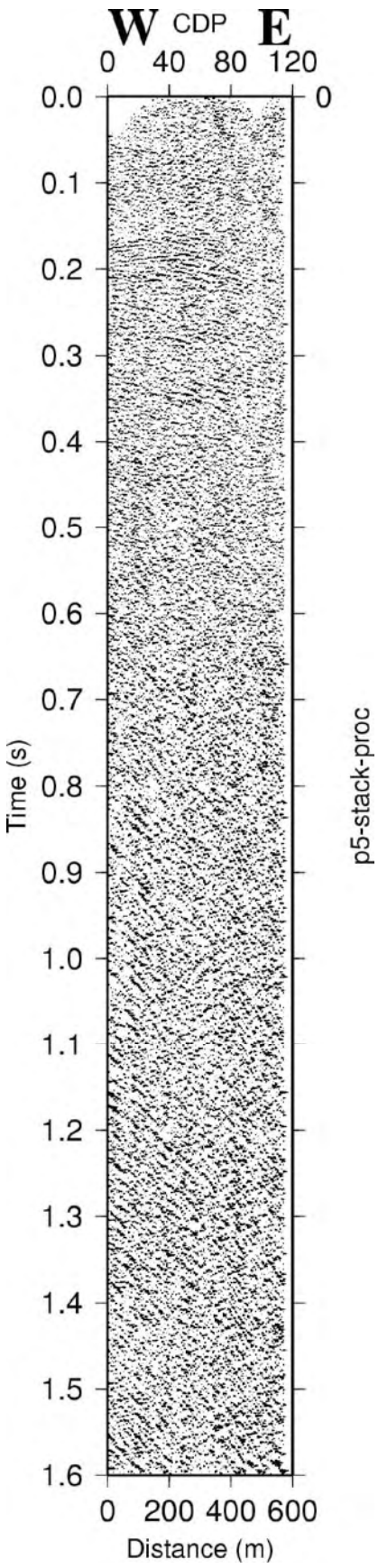

Figure 3-7. *Stacked section of profile 5 (LSM000199) down to 1.6 seconds.*

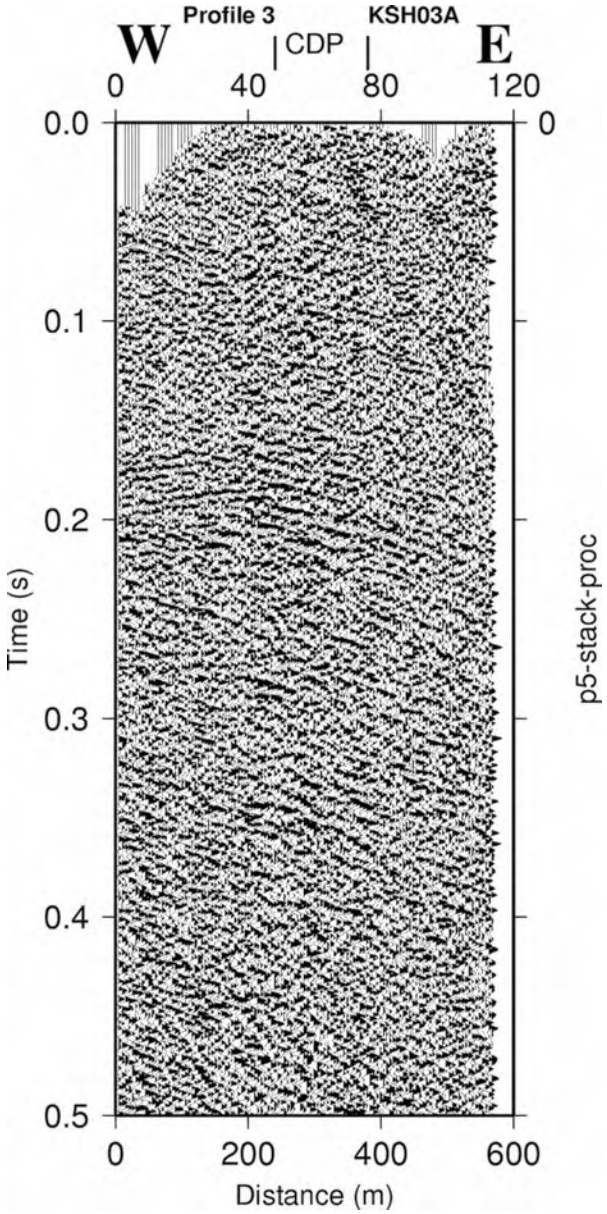

Figure 3-8. *Stacked section of profile 5 (LSM000199) down to 0.5 seconds.*

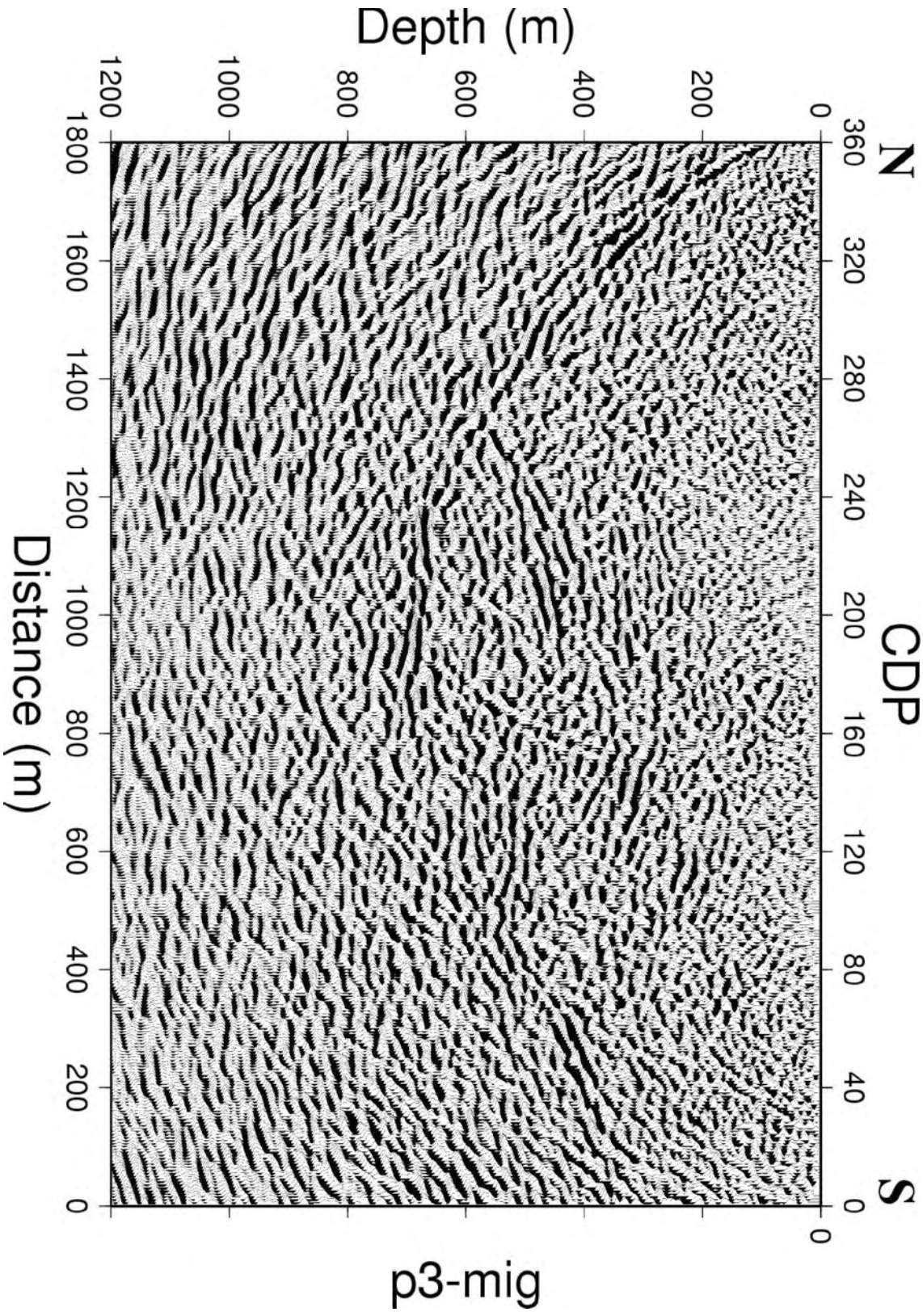

Figure 3-9. *Migrated section of profile 3 (LSM000197) down to 1200 m. Depth scale only valid for true sub-horizontal reflections.*

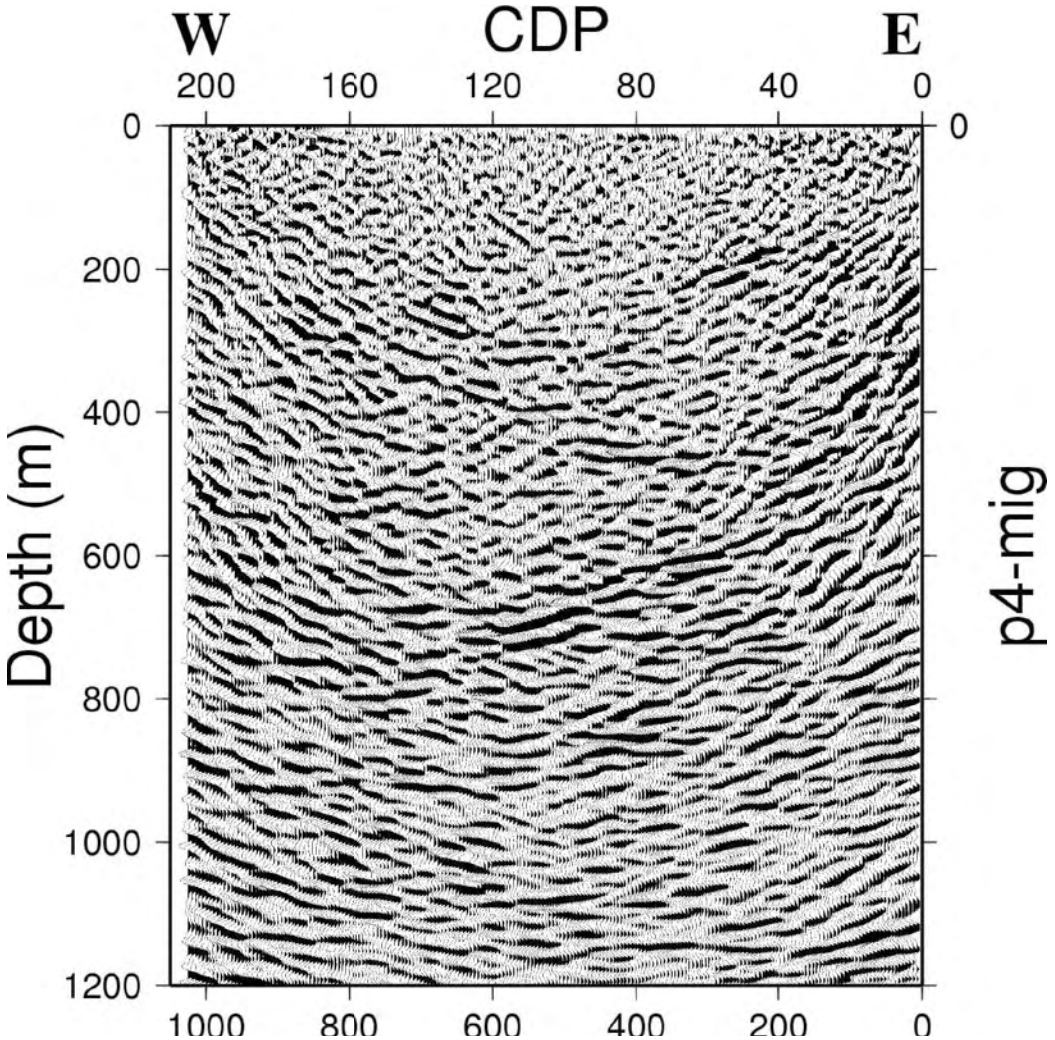

Figure 3-10. *Migrated section of profile 4 (LSM000198) down to 1200 m. Depth scale only valid for true sub-horizontal reflections.*

3.3 Array data

First breaks from the array (GSM000010) stations are used for estimating the bedrock velocity within the array area. Due to the relatively short offsets involved, velocity information as a function of depth is limited.

Use of the fixed array (GSM000010) also provides information on the variability of source amplitude and waveform along the profiles (Figure 3-11). Higher background noise is evident on shots fired on the southern and northern parts of profile 3 (LSM000197) and profile 5 (LSM000199). However, the first arrival amplitudes are generally high on shots fired along profile 5 (LSM000199) indicating that significant energy was transferred into the bedrock. Lowest noise levels are along the central parts of profile 3 (LSM000197) and profile 4 (LSM000198).

First breaks have been picked on the array (GSM000010) stations where the data quality were of sufficient quality. These first breaks plot nearly as a straight line as a function of offset (bottom part of Figure 3-12). When the first break times are reduced, a value of distance divided by velocity is subtracted, the data suggest that a velocity gradient exists in the upper few hundred meters of bedrock (top part of Figure 3-12). At offsets greater than 700 m the apparent velocity tends to flatten out at about 6 000 m/s. Results from the inversion of the first break traveltimes are presented in section 4.2.

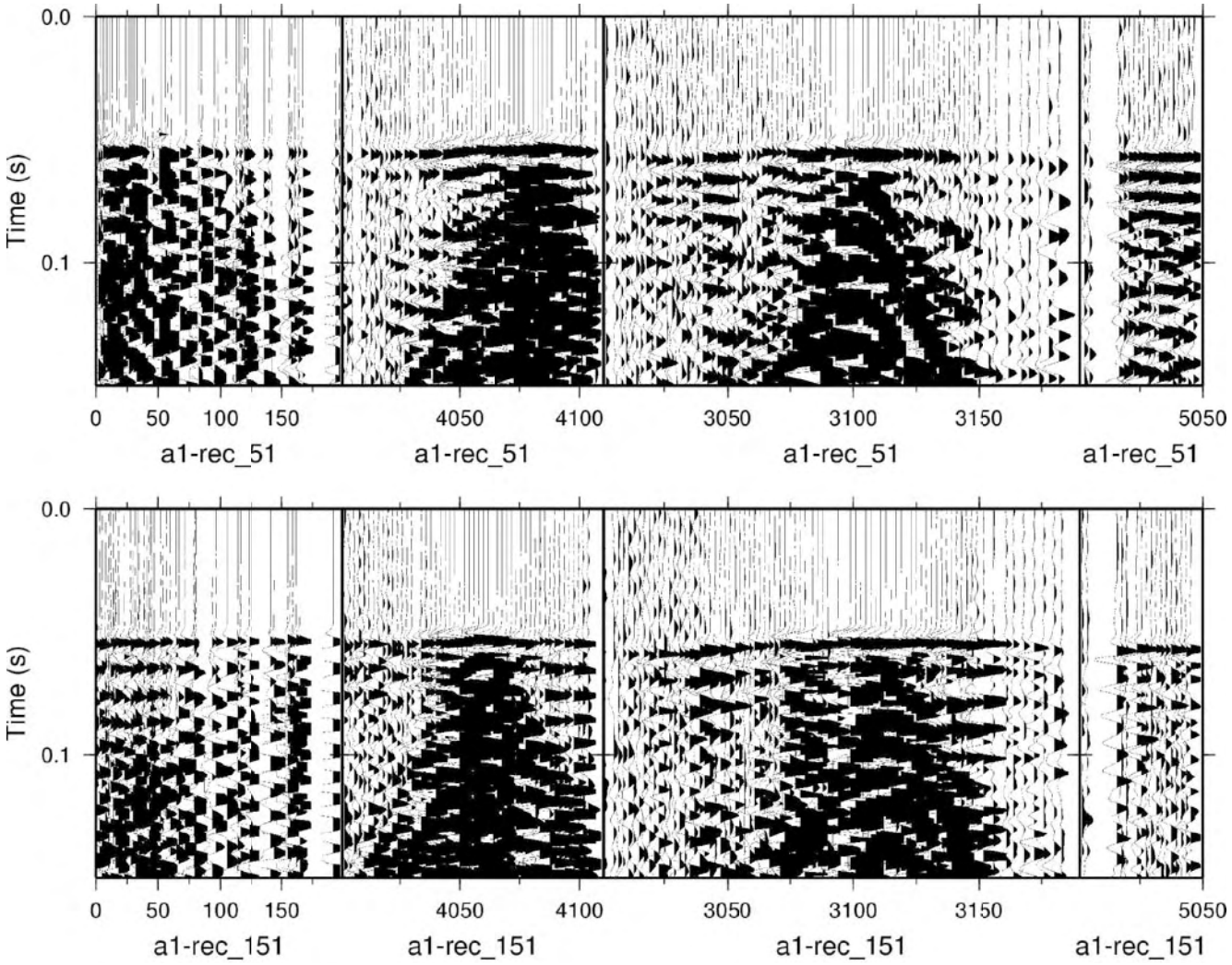

Figure 3-11. *Examples of two receiver gathers from within the fixed array (GSM000010). Data are grouped into shots fired in the array and along each profile. Scaling by time, linear moveout of 5 700 m/s and refraction statics have been applied prior to plotting. The same gain has been applied to all traces.*

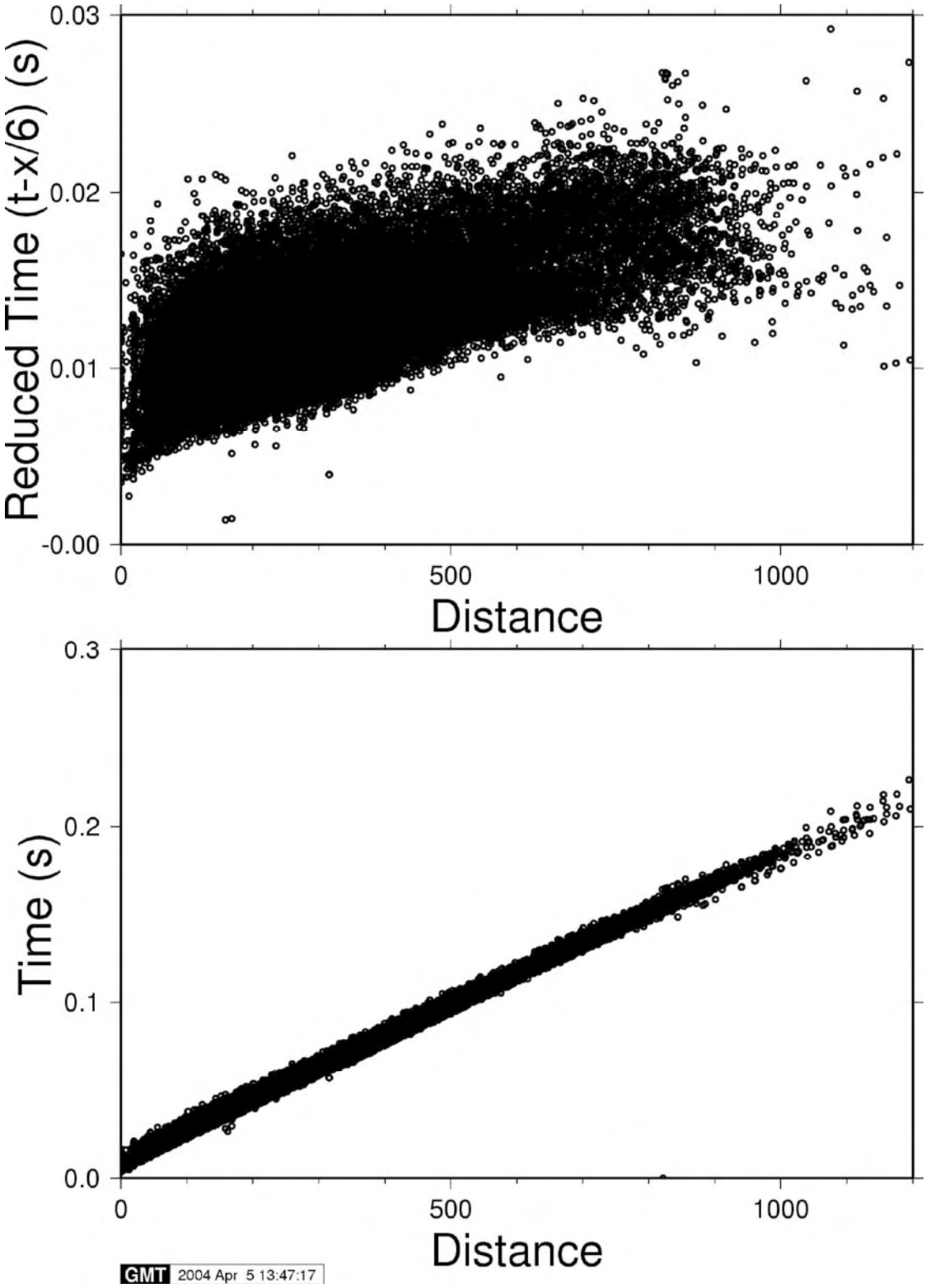

Figure 3-12. *Bottom – plot of all picked first breaks as a function of offset. Top –same data as bottom plot except that all picked first breaks have been reduced by 6 000 m/s. After reducing the first breaks a small velocity gradient appears to be present in the area.*

4 Interpretation

4.1 Reflection seismic

4.1.1 Background

An important aspect of high-resolution seismic studies for nuclear waste disposal is the three dimensional imaging of reflectors and their correlation with borehole data. Fracture zone geometry is often complex and highly three dimensional /8/. Ideally, 3D data should be acquired, but this is a very expensive solution. When only 2D data are available, it is only in the vicinity of crossing lines that it is possible to calculate the true strike and dip of reflectors. Also, if reflections project to the surface on single-line data and can be correlated with a surface feature at the intersection point, then an estimate of the strike and dip can also be made.

Inspection of the stacked sections (Figures 3-3 to 3-8) shows some high reflectivity in the upper 3–4 km of crust in parts of the survey area. These reflections may be due to the presence of fracture zones, mafic sheets (sills or dikes), mylonite zones or lithological boundaries at depth. Experience has shown that mafic sheets, in particular, generate distinct high amplitude reflections. Reflections from fracture zones are generally weaker and less distinct. Lateral changes in the reflectivity along the profiles may be due to changes in the geology, but also to changes in acquisition conditions. Noise from the Oskarshamn power plant, crooked lines /10/ and changes in the near surface conditions where the shots were fired may result in poorer images of reflections along some portions of the stacked sections.

4.1.2 General Observations

Profiles 3 (LSM000197) and 4 (LSM000198) show relatively higher reflectivity in the upper 0.4 s. At greater times the sections are relatively transparent. However, clear reflections are generally present at about 0.8 s and at 1.1 s (Figures 3-3 and 3-5) indicating that signal penetration was not a problem. These deep reflections were also observed on the Ävrö 1996 data /6,7/ and below the Laxemar area /3,4/. The lack of deeper reflections on profile 5 (LSM000199) (Figure 3-7) indicates that there are signal penetration problems along that profile.

4.1.3 Comparison with previous studies

It is useful to compare the present sections with those acquired earlier on Ävrö in 1996 /6,7/. Reflection geometry along profile 4 (LSM000198) and profile 1 from 1996 show similar geometries (Figure 4-1), as do geometries along profile 3 (LSM000197) and profile 2 from 1996 (Figure 4-2). Note that the frequency content of the data from 1996 is higher and that the signal to noise ratio is better. This is probably due to the larger charge size used during the acquisition, 100 g in 2 m deep shot holes. Weather conditions were also better during the 1996 survey. However, the general geometric agreement along the sub-parallel profiles suggest that similar structures have been imaged on both surveys.

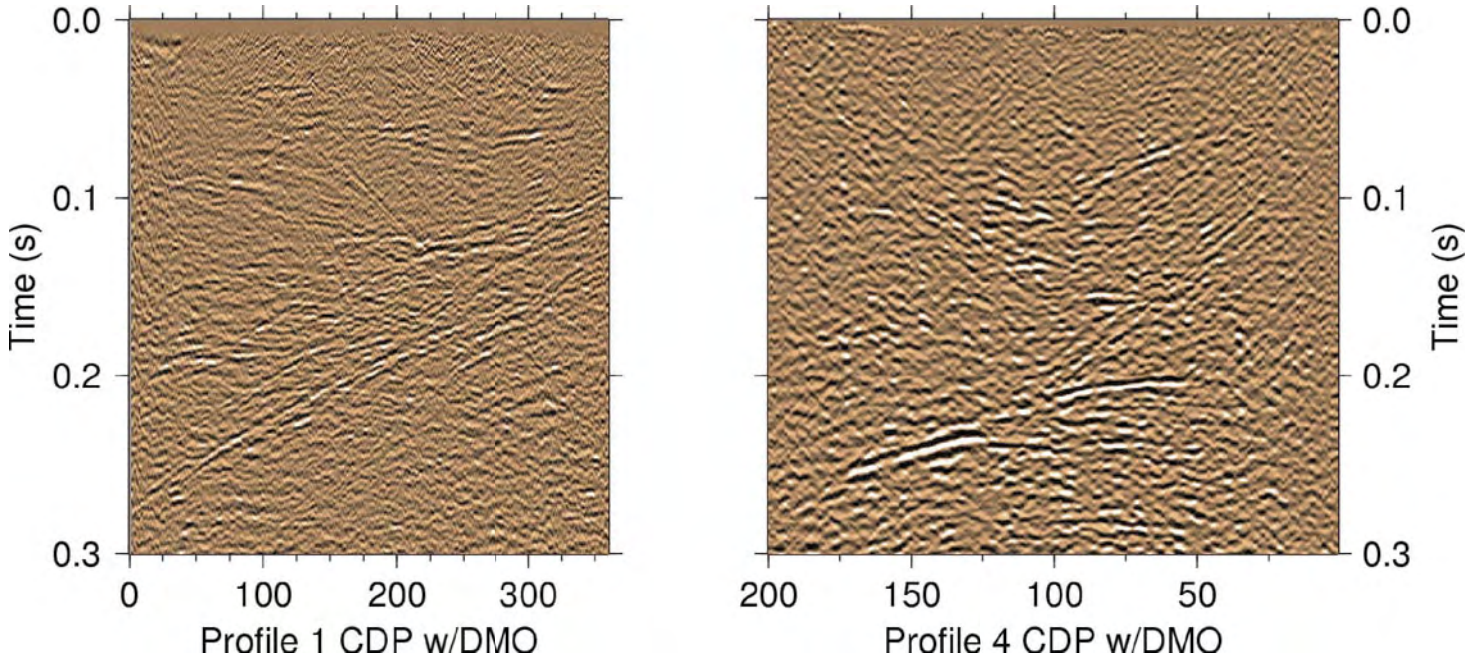

Figure 4-1. *Comparison of west-east running profile 1 from the Ävrö 1996 survey with west-east running profile 4 (LSM000198) from the present experiment.*

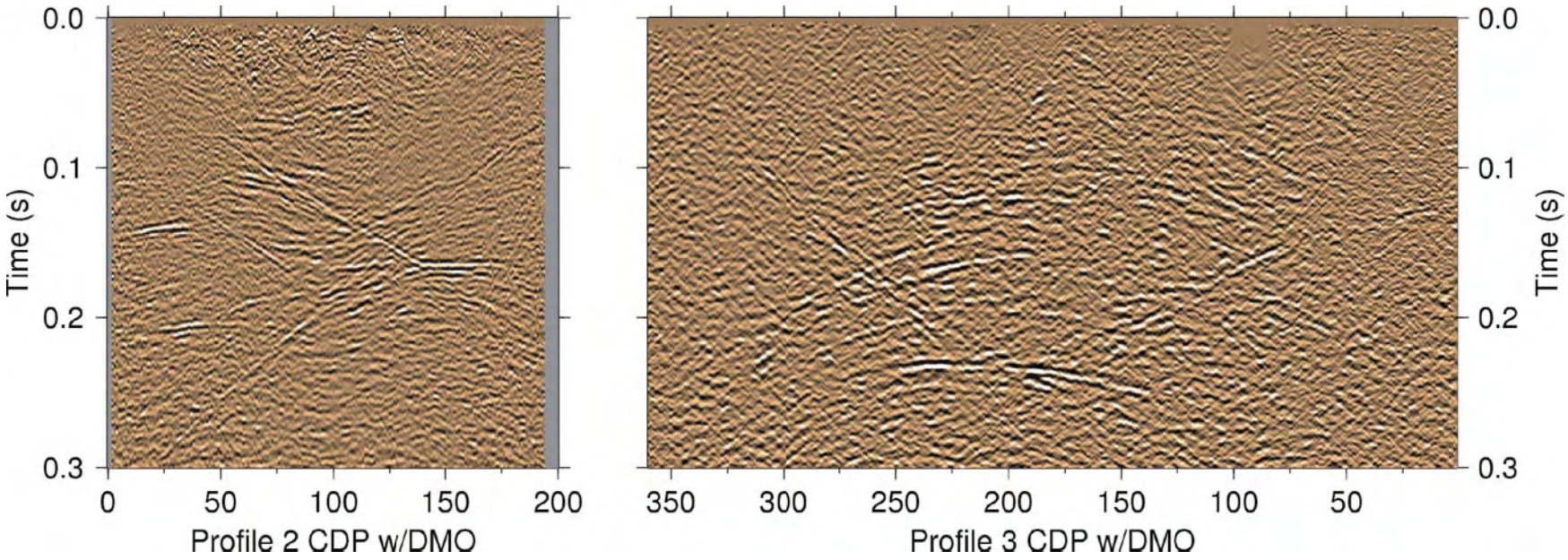

Figure 4-2. *Comparison of south-north running profile 2 from the Ävrö 1996 survey with south-north running profile 3 (LSM000197) from the present experiment.*

4.1.4 Seismic modelling and correlation between profiles

In order to obtain 3D control in the upper 1.5 km where the profiles cross, a combination of correlation of reflections between the profiles (Figures 4-3 to 4-6) and seismic modelling /1/ has been used. Note that the section shown for profile 5 (LSM000199) in these plots has been processed differently than the one in the previous chapter in order to enhance near-surface features that are observed on the shot sections. In principle, a reflection observed on one profile should be observed on a crossing profile at the crossing point at the same travel-time. This is not always the case on the present data set, especially for weaker reflections. Different reflections may have been enhanced in the processing on the different profiles. The crooked line acquisition may also result in destructive stacking of certain reflections, especially those coming from out-of-the-plane of the profile. Also, since numerous reflections are present on some parts of the profiles it can be difficult to uniquely identify one and the same reflection on two crossing profiles due to interference effects.

Table 4-1 lists those reflections that have been oriented and these are ranked according to the likelihood that the reflector would be encountered in a drilling operation. As a check on the picking and the orientation, reflections from these interfaces have been modelled (Figures 4-4 and 4-6), assuming that the interfaces are planes of infinite extent, and then compared with the observed data in order to obtain some idea of the lateral extent of the reflecting interfaces. When the reflection is not observed on the section or its position does not match that expected from the modelling, then the assumption of the reflector being an infinite plane has broken down. In Figures 4-4 and 4-6 reflections are labelled as defined in Table 4-1 and colour coded according to their rank. Note again that the red, blue and green lines are not picked reflections, but indicate on the seismic sections where the reflectors given in Table 4-1 are expected to appear if they correspond to planes of infinite extent.

Based on the orientation and amplitude of the reflections, four groups may be defined. These are group1 (reflections A1–A4) that strike parallel to the coast and dip landward at 20–50º, group 2 (reflections B1–B4 and G1–G2) which strike E-W and dip to the south at about 25–50º, group 3 (reflection E1) that is sub-horizontal and of high amplitude, and group 4 (reflections D1–D3) that are sub-horizontal and weak. Reflections A1 and B1 were observed on the Ävrö 1996 survey /6,7/.

4.1.5 Reflections which cannot be oriented

Most of the significant reflections can be oriented. However, there are some high amplitude reflections on profile 3 (LSM000197) (marked X in Figure 4-4) that cannot be uniquely oriented. These reflections are sub-parallel to the A2 reflection on profile 3 (LSM000197) and may be related to the A system. Alternatively, they may be sub-horizontal and originate from interfaces similar to that of the E1 reflection.

4.1.6 Reflections which have been picked for input into RVS

Raw data from the measurements were delivered directly after the termination of the field activities. The delivered data have been inserted in the database (SICADA) of SKB. The SICADA reference to the present activity is Field note No. 201. Coordinates for the reflecting elements which have been picked for input into RVS are shown in Figures 4-8 to 4-10. These reflecting elements have been provided for input into SICADA.

4.1.7 Projection of reflectors to surface

The reflections listed in Table 4-1 have been projected to the surface in Figure 4-7.

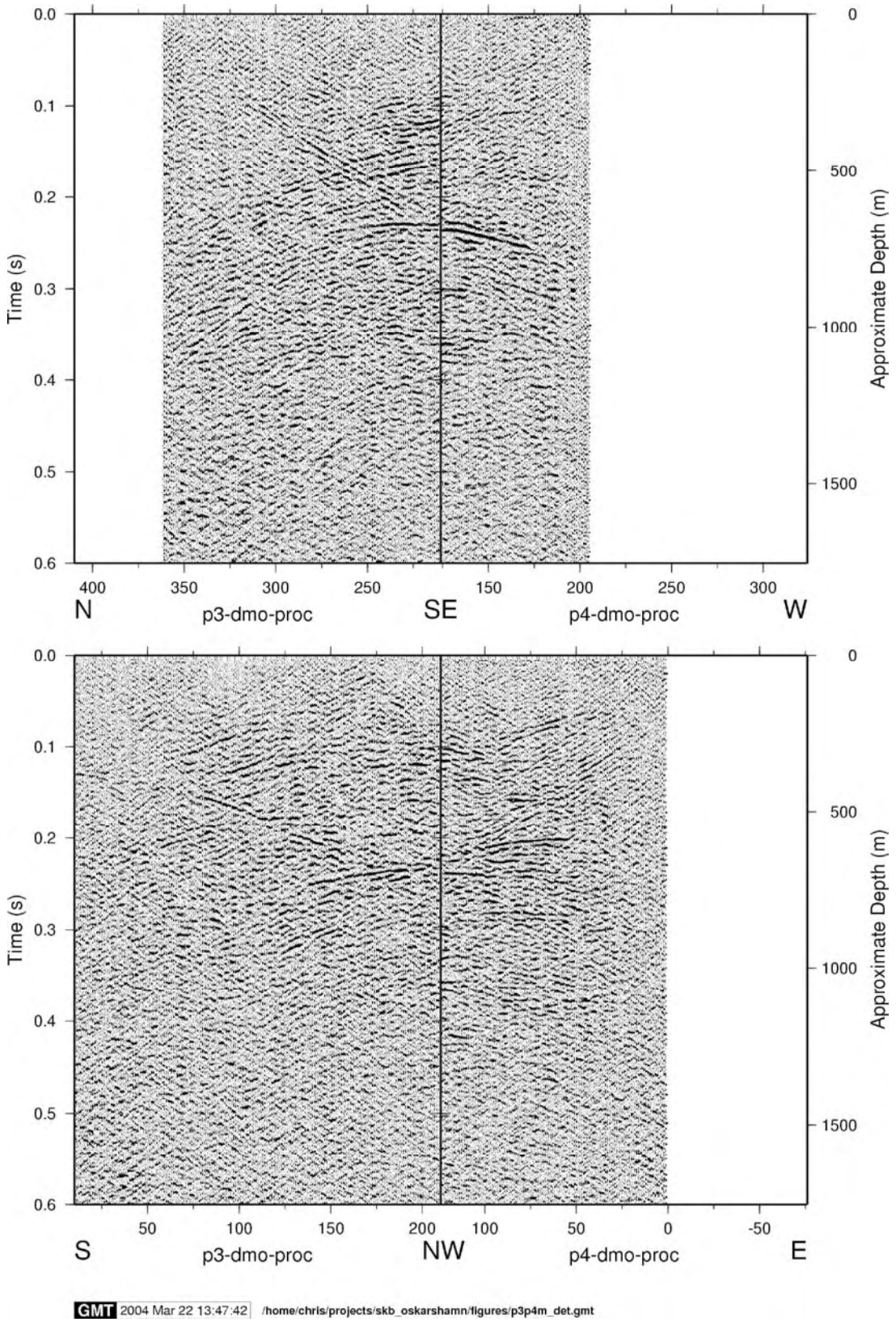

Figure 4-3. *Correlation of stacks from profiles 3 (LSM000197) and 4 (LSM000198) at their crossing point (Figure 3-1). Depth scale only valid for true sub-horizontal reflections. Horizontal numbering is CDP. Borehole KAV04 lies close to the crossing point.*

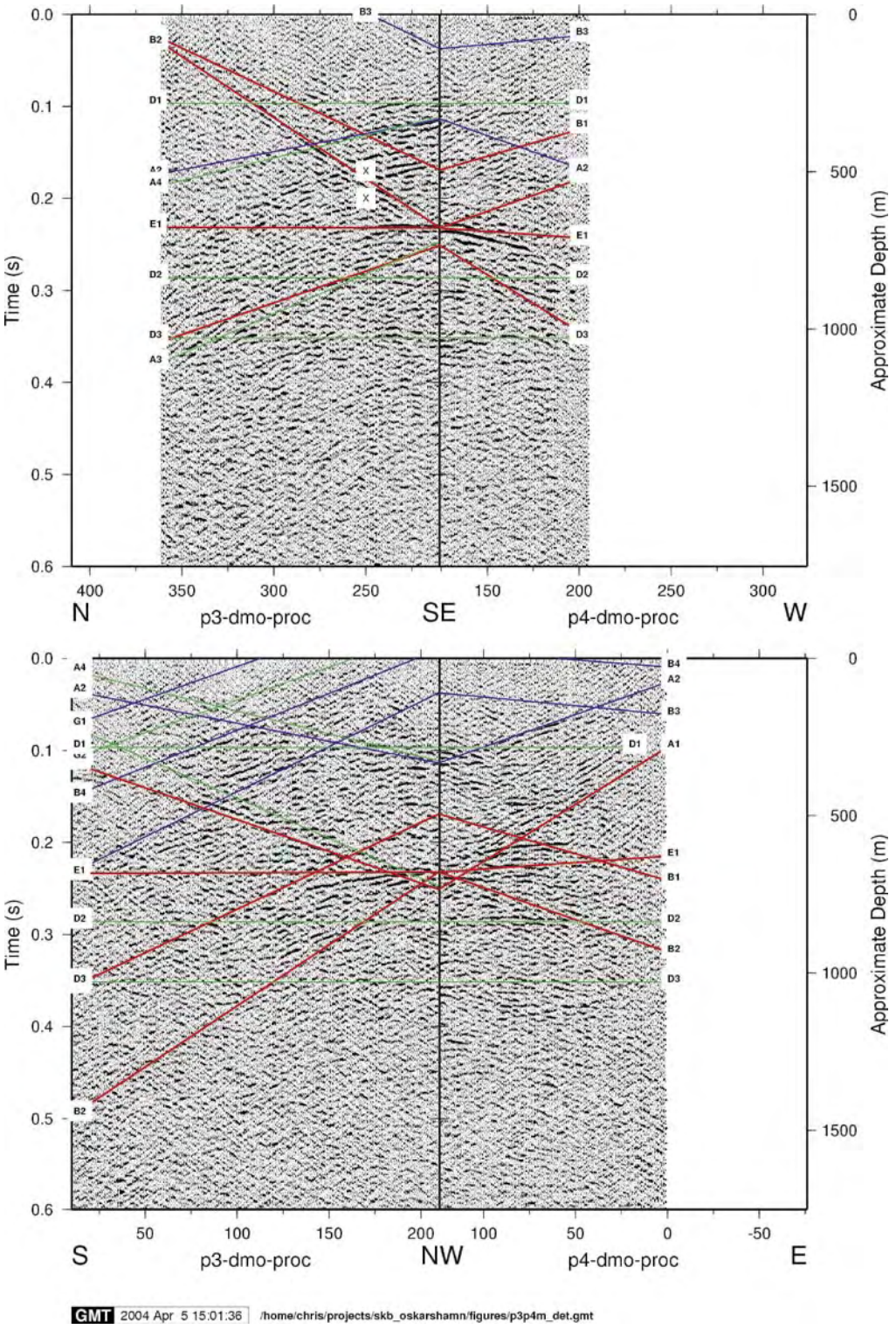

Figure 4-4. *Correlation of stacks from profiles 3 (LSM000197) and 4 (LSM000198) at their crossing point (Figure 3-1). Depth scale only valid for true sub-horizontal reflections. Horizontal numbering is CDP. Modeling of reflectors is coded as follows: red-rank 1, blue-rank 2, green-rank 3. Note that these lines are where reflections are expected to be observed on the seismic sections based on the strike and dips given in Table 4-1, they are* ***not*** *picked reflections. Borehole KAV04 lies close to the crossing point.*

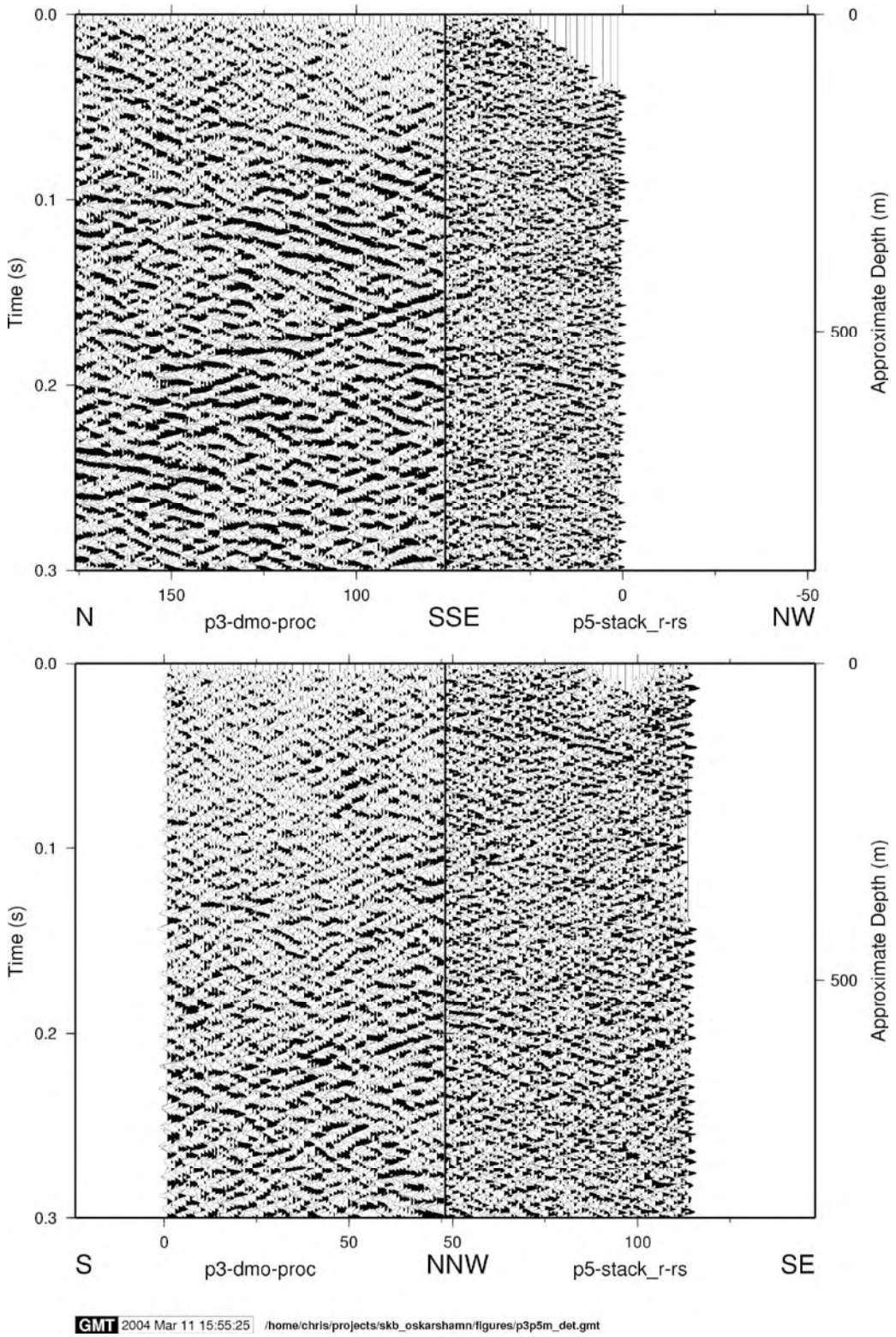

Figure 4-5. *Correlation of stacks from profiles 3 (LSM000197) and 5 (LSM000199) at their crossing point (Figure 3-1). Depth scale only valid for true sub-horizontal reflections. Horizontal numbering is CDP. A south dipping reflection is observed close to the surface.*

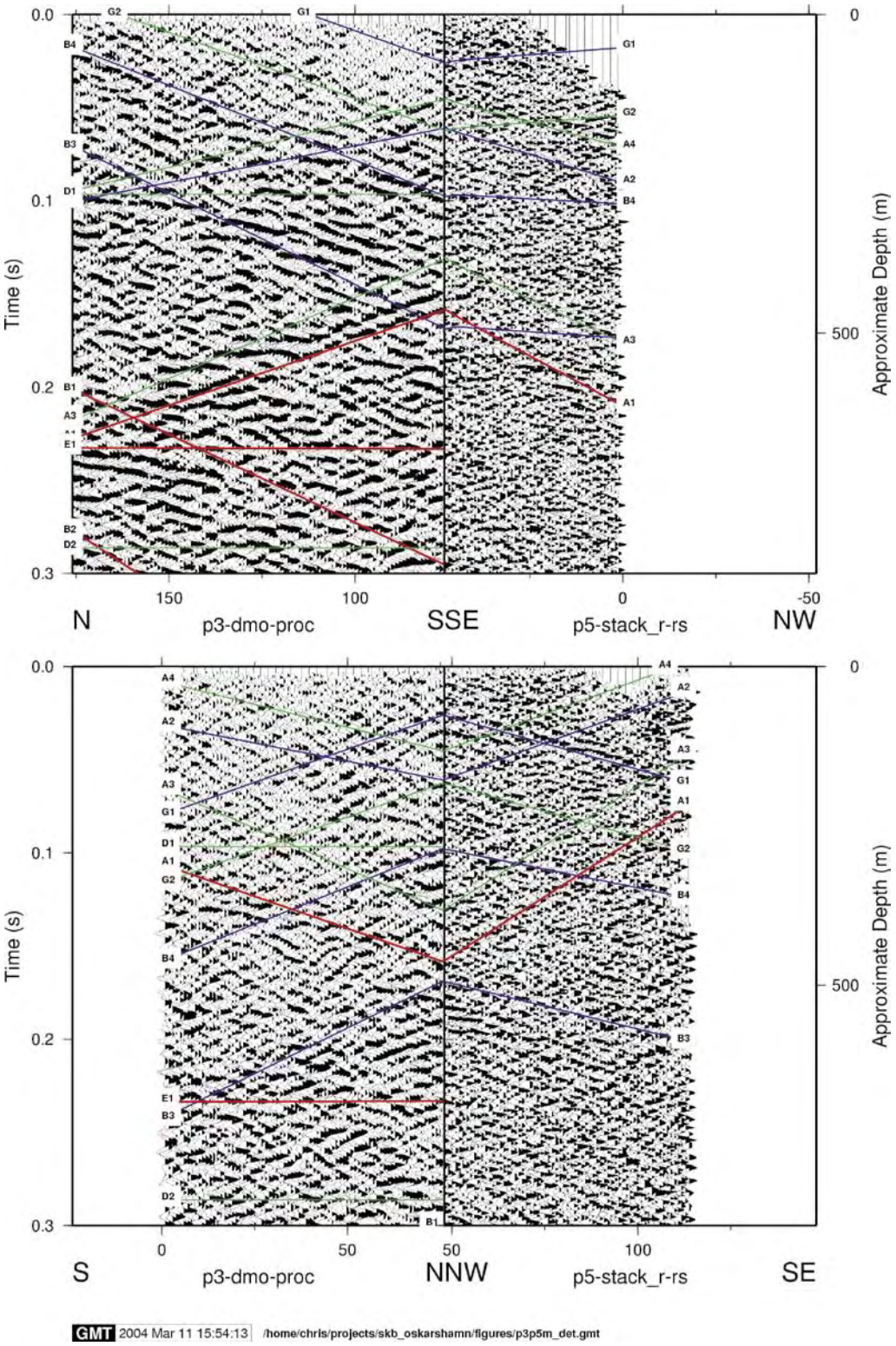

Figure 4-6. *Correlation of stacks from profiles 3 (LSM000197) and 5 (LSM000198) at their crossing point (Figure 3-1). Depth scale only valid for true sub-horizontal reflections. Horizontal numbering is CDP. Modelling of reflectors is coded as follows: red-rank 1, blue-rank 2, green-rank 3. Note that these lines are where reflections are expected to be observed on the seismic sections based on the strike and dips given in Table 4-1, they are not picked reflections.*

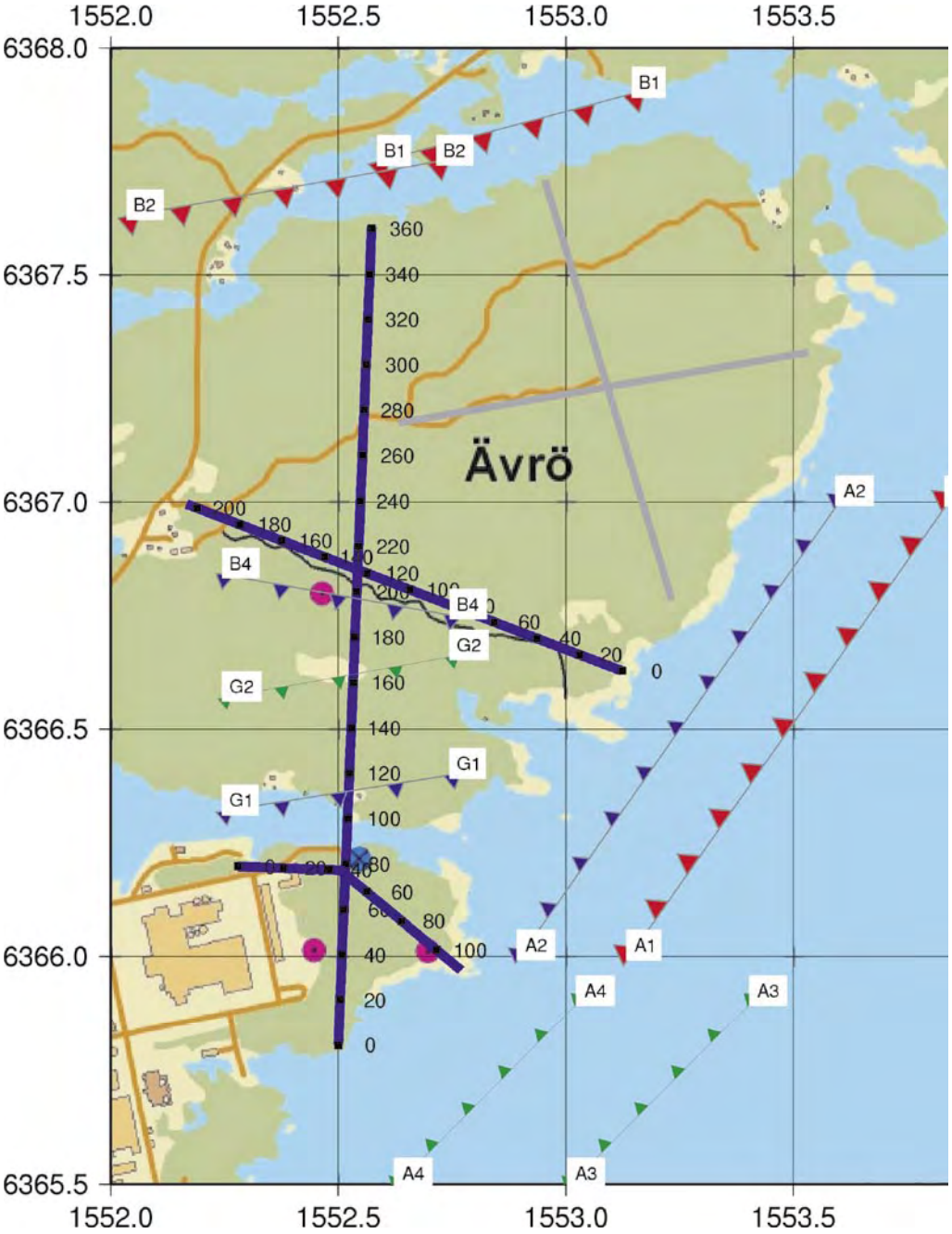

Figure 4-7. *Projected reflector intersections with the surface for those reflectors which project up to the surface. Reflections from interfaces that clearly cannot be traced to the surface, such as B3 and E1 in Table 4-1, are not drawn. Picked reflectors correspond to the tops of the reflector. Reflectors are coded as follows: red-rank 1, blue-rank 2, green-rank 3. Note that reflector B3 has not been plotted since it is difficult to trace this reflection to the surface.*

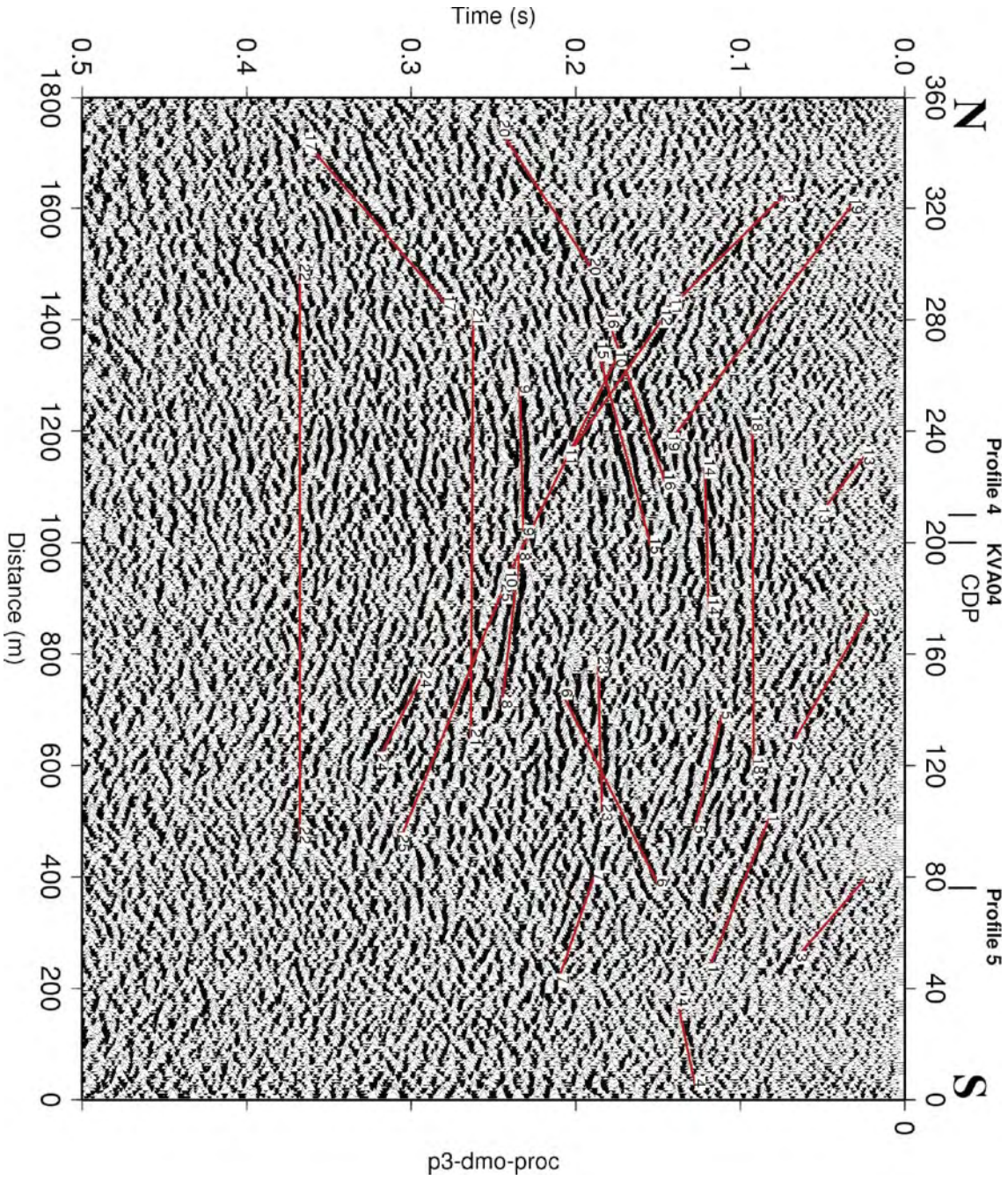

Figure 4-8. *Stacked section of profile 3 (LSM000197) down to 0.5 seconds with RVS picks.*

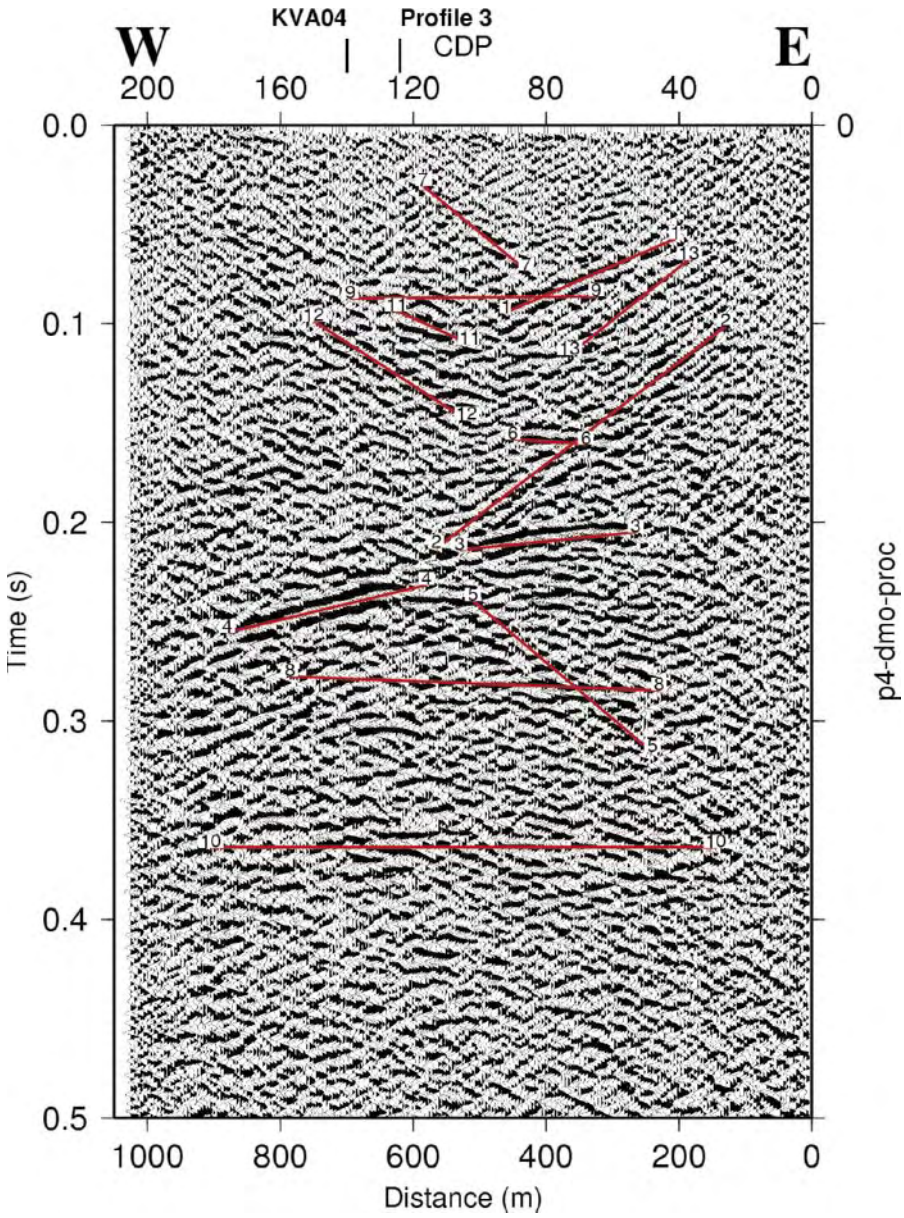

Figure 4-9. *Stacked section of profile 4 (LSM000198) down to 0.5 seconds with RVS picks.*

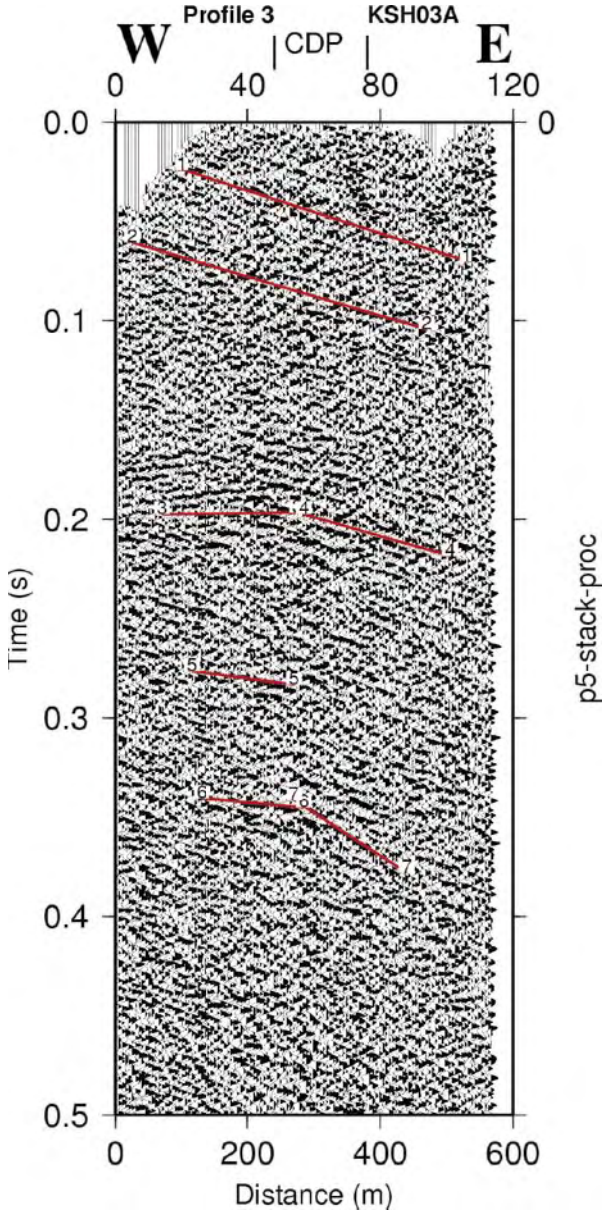

Figure 4-10. *Stacked section of profile 5 (LSM000199) down to 0.5 seconds with RVS picks.*

Table 4-1. Orientation of reflectors as determined from the surface seismic and partly shown in Figure 4-7. Reflectors may either be defined by distance to a point on the surface (better for dipping reflectors) or to by depth below this point (better for sub-horizontal reflectors). Distance refers to distance from the arbitrary origin (6367 km N, 1552.5 km W) to the closest point on the surface to which the reflector projects. Depth refers to depth below the surface at this origin. Strike is measured clockwise from north. Rank indicates how sure the observation of each reflection is on the profiles that the reflection is observed on; 1 – definite, 2- probable, 3-possible.

Reflector	Strike	Dip	Distance (m)	Depth (m)	Rank	Profiles observed on
B1	75	35	700		1	3, 4
B2	80	52	700		1	3, 4
B3	100	35	50		2	3, 4
B4	100	28	–200		2	3, 5?
A1	215	48	1100		1	3, 4, 5?
A2	215	25	900		2	3, 4, 5?
A3	225	20	1420		3	3?, 5?
A4	225	20	1150		3	3?, 5?
G1	80	25	–630		2	3, 5
G2	80	25	–380		3	3?, 5?
E1	180	5		680	1	3, 4
D1	90	0		300	3	3, 4
D2	90	0		830	3	3, 4
D3	90	0		1020	3	3, 4

4.1.8 Correlation with surface data

Topography

Group A reflections project to the surface in the sea and, therefore, no correlation with topography can be made. However reflections B1, B2 and B4 and G1 and G2 project to the surface where marked topographic lows are present (Figure 4-11). This correlation suggest that the source to these reflections are fracture zones.

Magnetics

Reflections G1 and G2 project to the surface where distinct magnetic lows are present (Figure 4-12). This further supports the suggestion that these reflections originate from fracture zones.

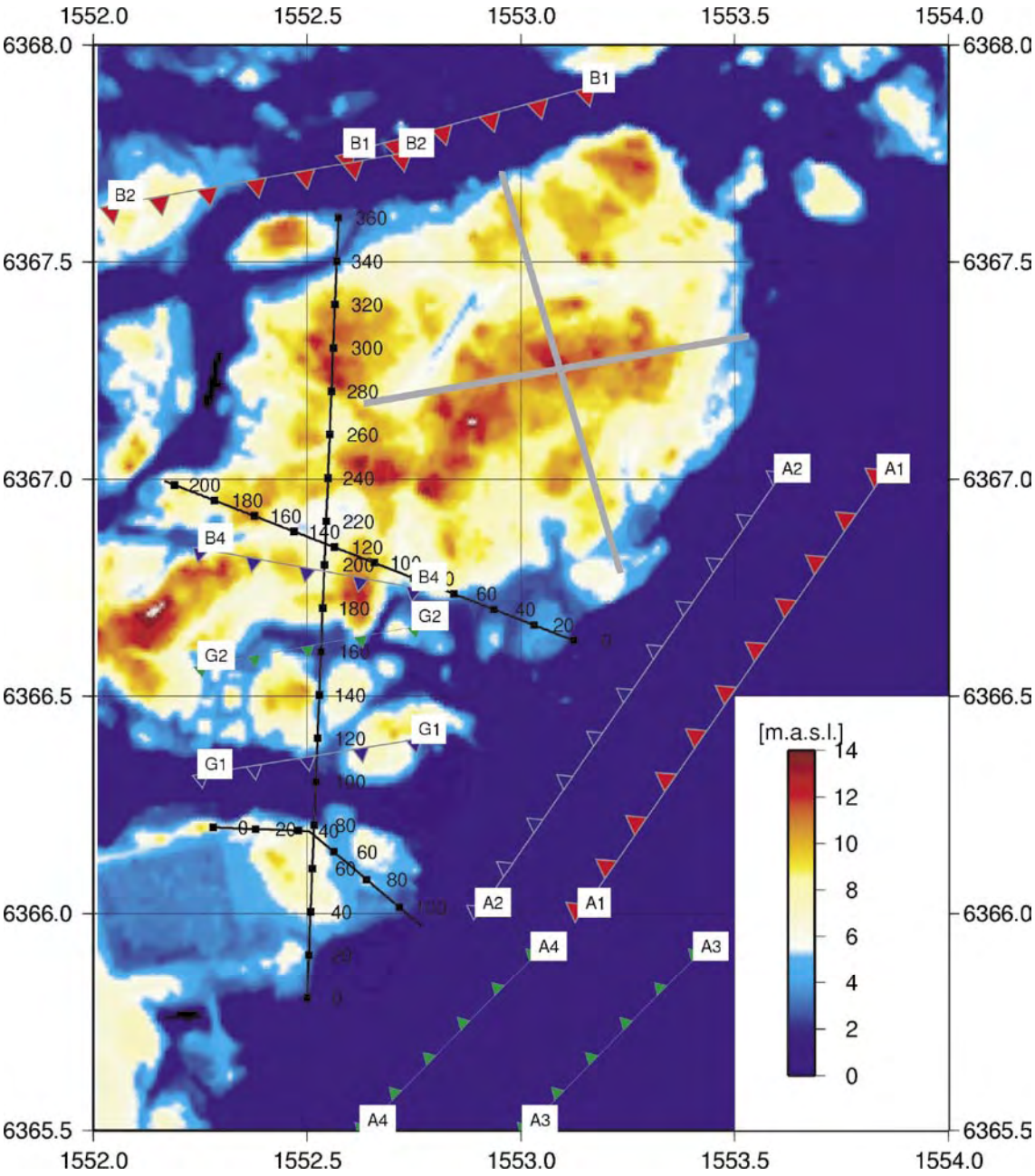

Figure 4-11. *Projected reflector intersections with the surface plotted on the topographic map. Reflections from interfaces that clearly cannot be traced to the surface, such as B3 and E1 in Table 4-1, are not drawn. All indicated reflectors are interpreted to correspond to relatively thin zones (5–15 m thick). Reflectors are coded as follows: red-rank 1, blue-rank 2, green-rank 3.*

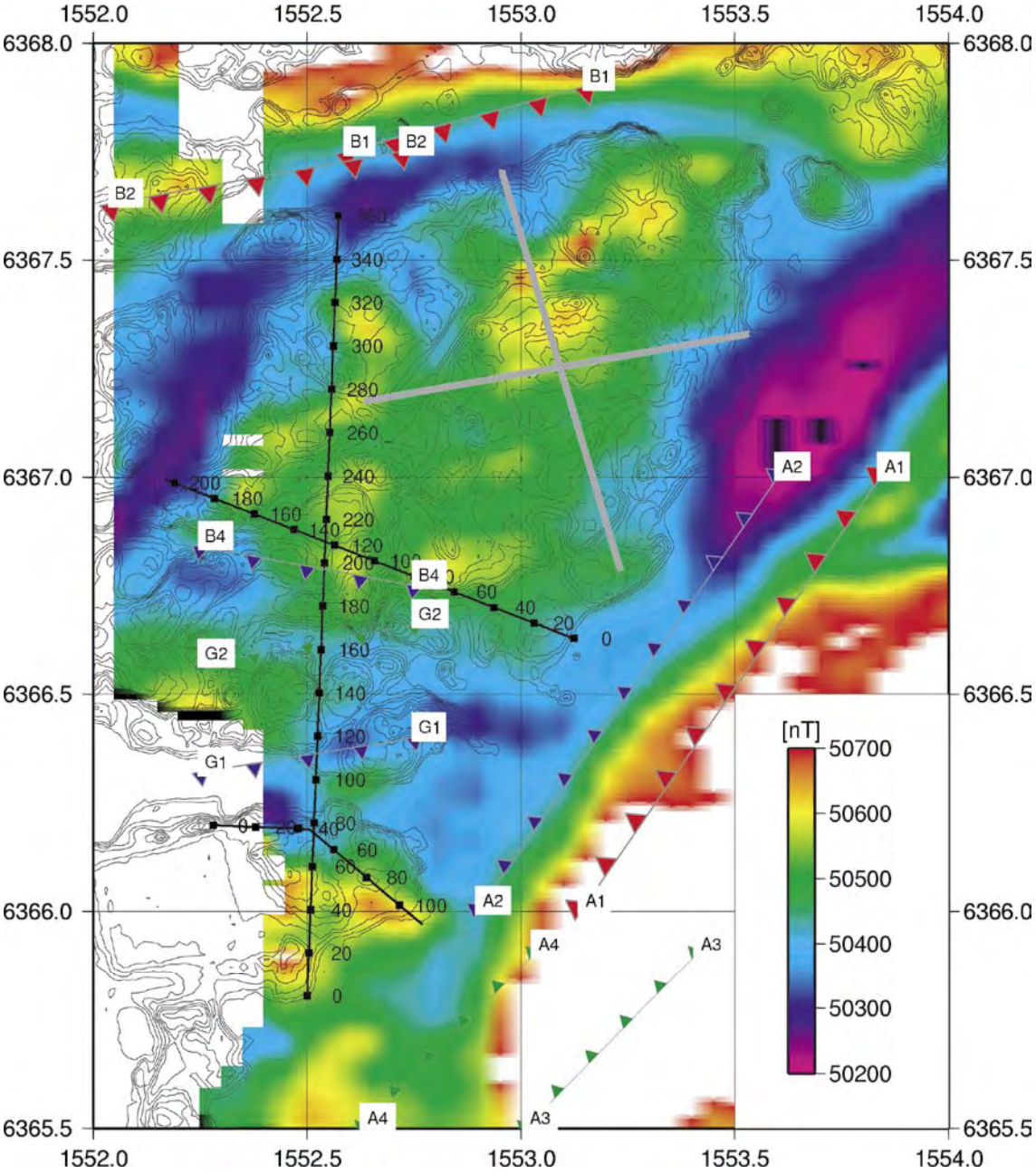

Figure 4-12. *Projected reflector intersections with the surface plotted on the total field magnetic map. Reflections from interfaces that clearly cannot be traced to the surface, such as B3 and E1 in Table 4-1, are not drawn. All indicated reflectors are interpreted to correspond to relatively thin zones (5–15 m thick). Reflectors are coded as follows: red-rank 1, blue-rank 2, green-rank 3.*

4.2 Tomography within the array

A preliminary 1D velocity model for the Ävrö area based on the array (GSM000010) first arrival traveltimes is shown in Figure 4-13. This velocity model was the starting point for estimating 3D velocity models using a LSQR based inversion code /2/ and /9/. An initial 3D model is determined by using the differences between predicted traveltimes through the 1D model and observed traveltimes (Figure 4-14). Once a satisfactory initial 3D model is obtained, the model is refined by repeating the inversion procedure to produce updated 3D velocity models resulting in a better velocity model fit (Figure 4-14). Results after 10 iterations of this procedure are shown in Figure 4-15. Inspection of Figure 4-15 shows that low velocity zones in the bedrock tend to strike in E-W direction, the same general strike as the B and G sets of reflections. Reflector G2 projects to the surface on top of a marked low velocity zone. This low velocity zone lies outside of the array (GSM000010), but its location coincides with the marked topographic low noted earlier.

A by-product from the inversion method used is the receiver static /5/. This gives a delay time at each geophone in the receiver array. These delay times are proportional to the thickness of the overburden and, thus, depth to bedrock. The receiver static image indicates E-W striking structures are present below the array (GSM000010) (Figure 4-16).

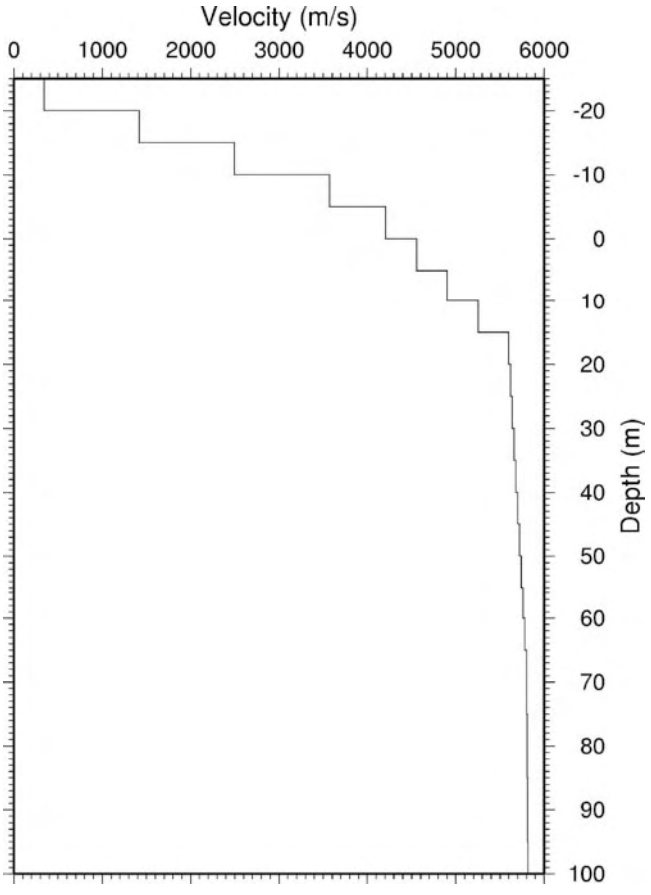

Figure 4-13. *Initial 1D P-wave velocity model for the Ävrö area based on first arrival times from the array stations.*

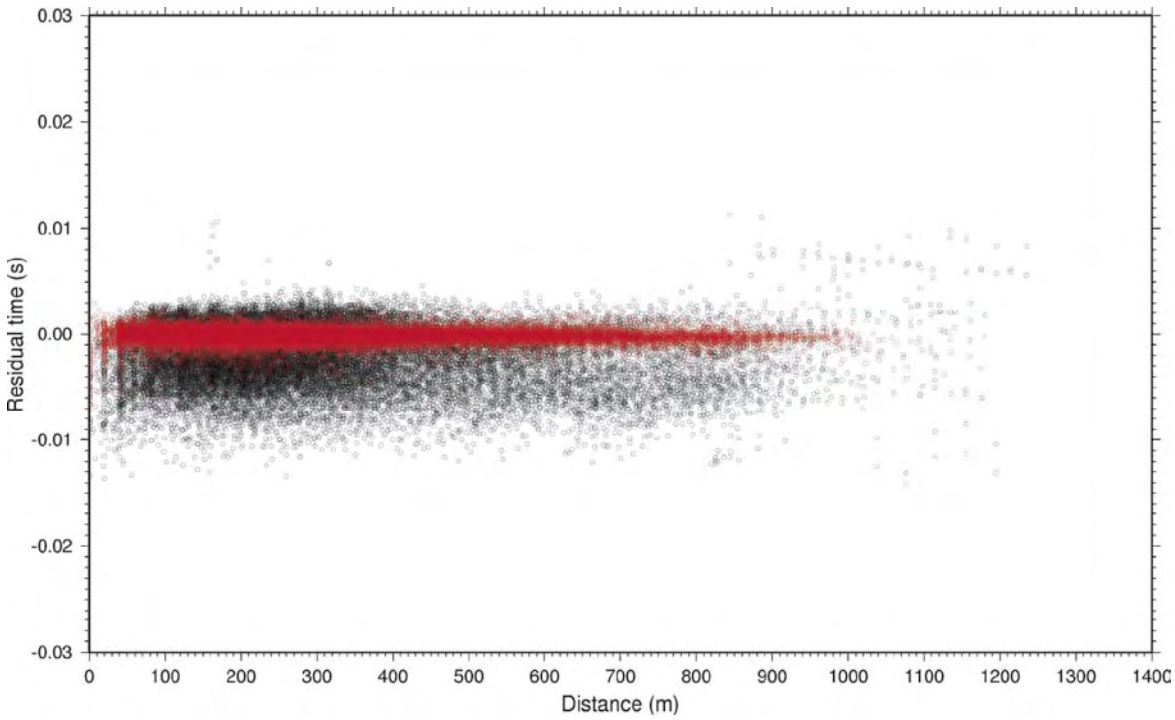

Figure 4-14. *Comparison of the residuals of the modeled first arrival times minus the observed first arrival times for the initial model in Figure 4-13 (black circles) compared to the residuals from the final model (red circles). The final model fits the data much better then the initial model. Distance refers to the source receiver offset.*

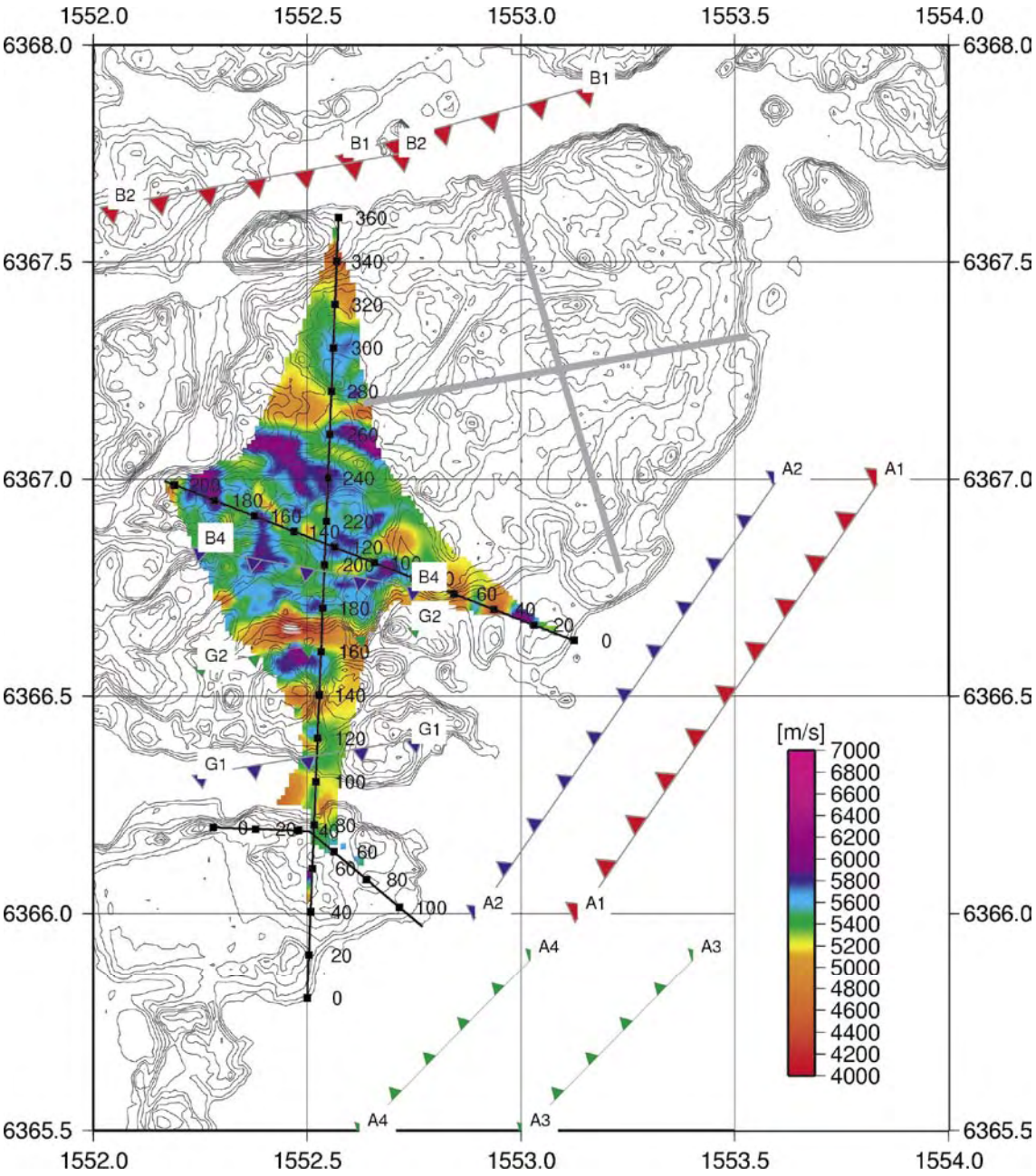

Figure 4-15. *Plan view of the 3D tomography results in the depth interval 10–15 m. Reflections from interfaces that clearly cannot be traced to the surface, such as B3 and E1 in Table 4-1, are not drawn. All indicated reflectors are interpreted to correspond to relatively thin zones (5–15 m thick). Reflectors are coded as follows: red-rank 1, blue-rank 2, green-rank 3.*

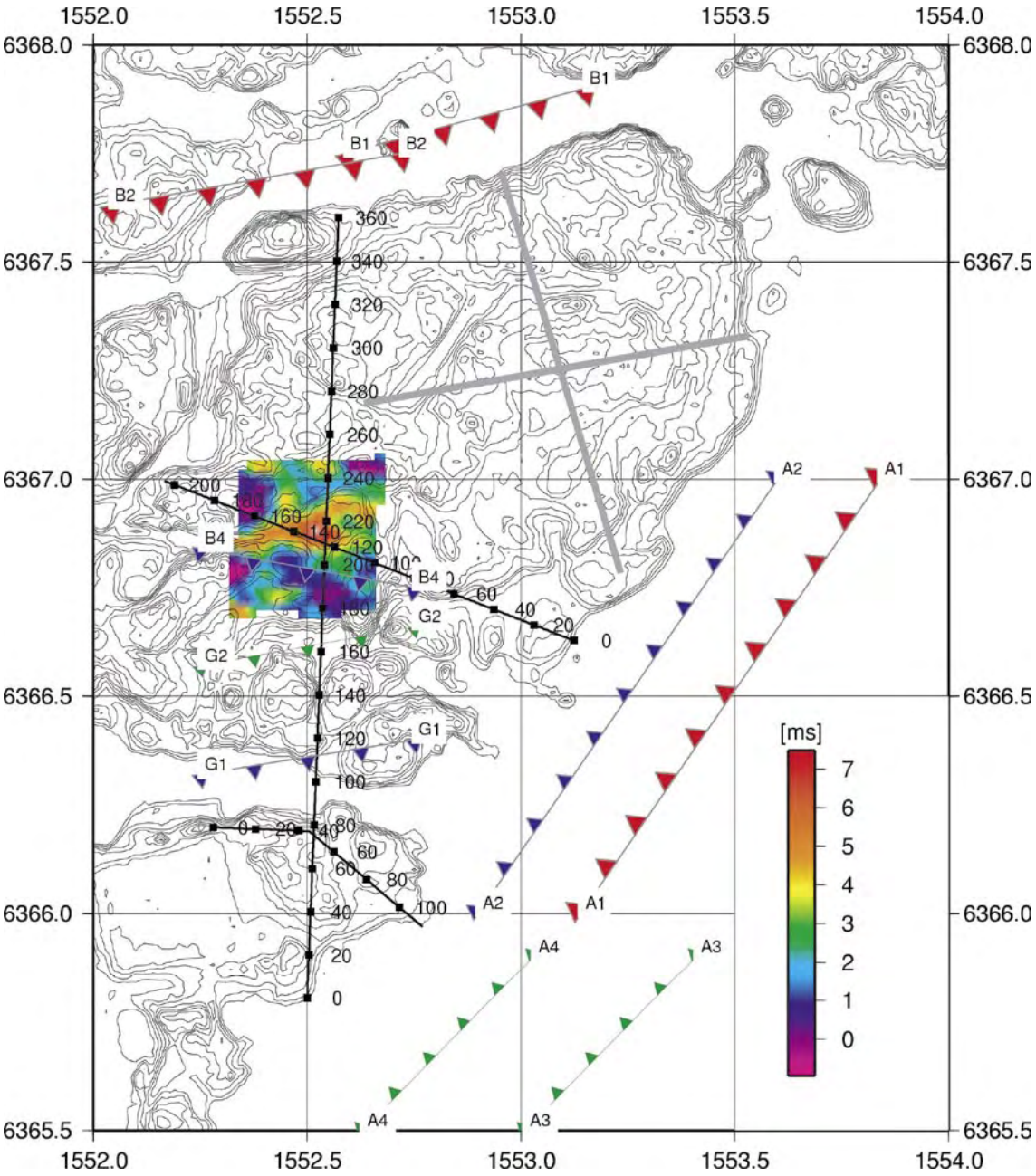

Figure 4-16. *Receiver static delay for each station within the array (GSM000010). Higher delays indicate depth to bedrock is greater. Reflections from interfaces that clearly cannot be traced to the surface, such as B3 and E1 in Table 4-1, are not drawn. All indicated reflectors are interpreted to correspond to relatively thin zones (5–15 m thick). Reflectors are coded as follows: red-rank 1, blue-rank 2, green-rank 3.*

4.3 Predictions for deep borehole KAV04

Intersection points of the picked reflectors with the projection of borehole KAV04 downwards are given in Table 4-2. The only reflectors of rank 1, the most reliably identified reflections, that are expected to be penetrated by the 1000 m deep borehole are the south dipping B1 reflection that is best imaged on the Ävrö 1996 survey and the sub-horizontal E1 reflection. Note that the depths are very approximate and most reliable for sub-horizontal reflectors.

Table 4-2. Predicted intersection points of KAV04 with those reflectors that project into the borehole shallower than 1 500 m. Rank indicates the quality of the prediction; 1- highly likely, 2- probable, 3-possible. Note that these depths differ from those in Table 4-1 since the origin for the orientation (6367 km N, 1552.5 km W) is not coincident with the borehole. Depths to reflectors also differ from the approximate depths given in Figures 4-4 and 4-6 since these are time sections and many of the reflections are dipping and from out-of-the plane of the profiles. Only sub-horizontal reflections will have correct approximate depths.

Reflector	Intersection depth (m)	Strike	Dip	Rank
B1	630	75	35	1
B2	1150	80	52	1
B3	190	100	35	2
B4	10	100	28	2
A1	1130	215	48	1
A2	380	215	25	2
A3	480	225	20	3
A4	380	225	20	3
E1	690	180	5	1
D1	300	90	0	3
D2	830	90	0	3
D3	1020	90	0	3

5 Discussion and conclusions

5.1 Acquisition

Acquired data were of variable quality compared to the Ävrö 1996 /6,7/ and Laxemar 1999 /3,4/ surveys. A larger charge size fired in deeper shot holes was used in the Ävrö 1996 survey. This partly explains the better quality of the data from that survey. However, weather conditions were also better during the Ävrö 1996 survey. The same source parameters were used on the Laxemar 1999 survey as on the present survey. The difference in data quality is probably due to Laxemar being further inland, further from the Oskarshamn power plant and that the data were also acquired under better weather conditions. Although the data quality are poorer on the present survey, the quality is sufficient to for imaging the upper kilometre of the crust. There is no reason to change the source parameters for future surveys that will use an explosive source.

5.2 Processing

Stacked sections on the Simpevarp peninsula do not show clear reflections. The proximity of the power plant certainly affects the data quality, however, it is not noise from the power plant which is the main detriment to producing a high quality stacked section. Some processed shot and receiver gathers show clear reflections from the upper 500 m of crust (Figure 5-1) demonstrating the presence of reflecting interfaces near the surface. The lack of clear reflections on the stacked section is probably due to the lower fold in this area and the limited offsets available for stacking. Earlier studies in the Siljan Ring area have shown that one of the most important parameters for obtaining high quality sections of the upper crust is high fold. There are two ways to increase the fold, add more channels or shoot more often. In the Simpevarp peninsula only about 50 channels were effectively recording data in the area during acquisition due to the small size of the area. The only way to add more channels to increase the fold is by reducing the shot and/or receiver spacing on. Reducing shot and receiver spacing to 5 m would increase fold by 2 if the same maximum offset is retained. Increasing maximum offset is not possible due the geometrical limits of the area being surveyed.

5.3 Interpretation

Both the reflection seismic data (LSM000197, LSM000198 and LSM000199) and array (GSM000010) data indicate several E-W striking structures on the island of Ävrö, some of which can be correlated to topographic and magnetic lows. The reflection data indicate that these E-W striking zones dip at about 25–50 to the south (groups B and G). In addition, there are reflectors which dip at 20–50º to the northwest that project up to the surface offshore of the island of Ävrö and parallel (SW-NE) to its coast (group A). Both these sets are interpreted to correspond to fracture zones. A strong sub-horizontal reflector at about 700 m depth below the centre of the island of Ävrö may be a mafic lens. Weaker sub-horizontal reflections may originate from fracture zones, but these have not been well imaged. There are a few strong gently dipping reflections along the profiles that cannot be

oriented. Data from the Simpevarp peninsula are difficult to interpret due to the low fold and limited offset range of the acquisition. Therefore, the orientation of these reflectors is less well constrained in this area. However, both the E-W striking and SW-NE striking sets of reflectors appear to be present below the peninsula.

5.4 Recommendations

Based on the results from the present survey the following recommendations are made:

- For lines shorter than 1 km a station spacing of 5 m should be used.
- For lines shorter than 500 m a station spacing of 3 to 4 m should be considered.

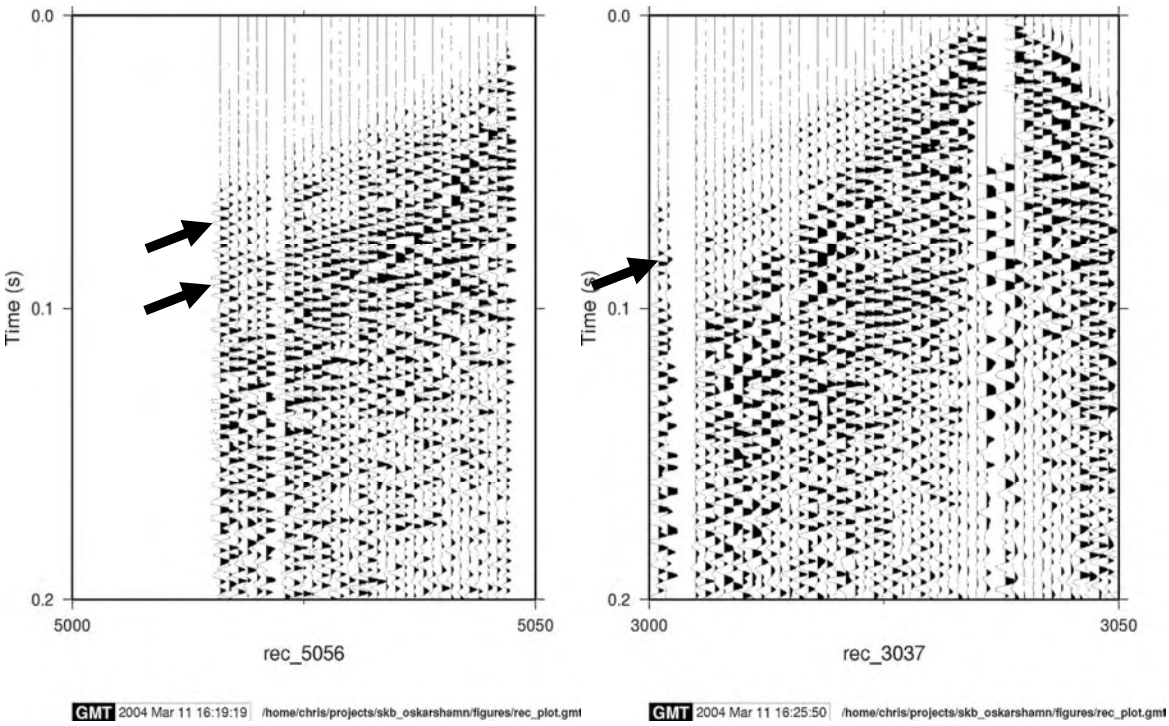

Figure 5-1. *Processed receiver gathers from Simpevarp peninsula from profile 5 (LSM000199) (left) and profile 3 (LSM000197) (right). Arrows mark clear reflections.*

References

/1/ Ayarza P, Juhlin C, Brown D, Beckholmen M, Kimbell G, Pechning R, Pevzner L, Pevzner R, Ayala C, Bliznetsov M, Glushkov A, Rybalka A, 2000. Integrated geological and geophysical studies in the SG4 borehole area, Tagil Volcanic Arc, Middle Urals: Location of seismic reflectors and source of the reflectivity, J. Geophys. Res.: 105, 21333–21352.

/2/ Benz H M, Chouet B A, Dawson P B, Lahr J C, Page R A, Hole J A, 1996. Three-dimensional P and S wave velocity structure of Redoubt Volcano, Alaska. J. Geophys. Res.: 101, 8111–8128.

/3/ Bergman B, Juhlin C, Palm H, 2002. Reflection seismic imaging of the upper 4 km of crust using small charges (15–75 grams) at Laxemar, southeastern Sweden. Tectonophysics, 355, 201–213.

/4/ Bergman B, Juhlin C, Palm H, 2001. Reflektionsseismiska studier inom Laxemarområdet. R-01-07 (in Swedish). Svensk Kärnbränslehantering AB.

/5/ Bergman B, Tryggvason A, Juhlin C, 2004. High resolution seismic traveltime tomography incorporating static corrections applied to a till covered bedrock environment. In press, Geophysics.

/6/ Juhlin C, Palm H, 1999. 3D structure below Ävrö island from high resolution reflection seismic studies, southeastern Sweden. Geophysics: 64, 662–667.

/7/ Markström I, Stanfors R, Juhlin C, 2001. Äspölaboratoriet. RVS-modellering, Ävrö. Slutrapport. R-01-06 (in Swedish). Svensk Kärnbränslehantering AB.

/8/ Tirén S A, Askling P, Wänstedt S, 1999. Geologic site characterization for deep nuclear waste disposal based on 3D visualization. Engineering Geology: 52, 319–346.

/9/ Tryggvason A, Rognvaldsson S T, Flovenz O G, 2002. Three-dimensional imaging of the P and S wave velocity structure and earthquake locations beneath southwest Iceland. Geophysical J. Int.: 151, 848–866.

/10/ Wu J, Milkereit B, Boerner D, 1995. Seismic imaging of the enigmatic Sudbury structure. J. Geophys. Res.: 100, 4117–4130.